Hydrogeology Journal (2015) 23: 915–934
DOI 10.1007/s10040-015-1252-3

Time constant of hydraulic-head response in aquifers subjected to sudden recharge change: application to large basins

Guy Vasseur · Pauline Rousseau-Gueutin · Ghislain de Marsily

Abstract Analytical formulae are proposed to describe the first-order temporal evolution of the head in large groundwater systems (such as those found in North Africa or eastern Australia) that are subjected to drastic modifications of their recharge conditions (such as those in Pleistocene and Holocene times). The mathematical model is based on the hydrodynamics of a mixed-aquifer system composed of a confined aquifer connected to an unconfined one with a large storage capacity. The transient behaviour of the head following a sudden change of recharge conditions is computed with Laplace transforms for linear one-dimensional and cylindrical geometries. This transient evolution closely follows an exponential trend $\exp(-t/\tau)$. The time constant τ is expressed analytically as a function of the various parameters characterizing the system. In many commonly occurring situations, τ depends on only four parameters: the width a_c of the main confined aquifer, its transmissivity T_c, the integrated storage situated upstream in the unconfined aquifer $M=S_u a_u$, and a curvature parameter accounting for convergence/divergence effects. This model is applied to the natural decay of large aquifer basins of the Sahara and Australia following the end of the mid-Holocene humid period. The observed persistence of the resource is discussed on the basis of the time constant estimated with the system parameters. This comparison confirms the role of the upstream water reserve, which is modelled as an unconfined aquifer, and highlights the significant increase of the time constant in case of converging flow.

Keywords Analytical solution · Climate change · Groundwater flow · Time constant · Groundwater recharge/water budget

Received: 3 October 2014 / Accepted: 9 March 2015
Published online: 24 April 2015

G. Vasseur (✉) · G. Marsily
Sorbonne Universités, UPMC Univ. Paris 06, CNRS, EPHE, UMR 7619 METIS, 4 place Jussieu, F75005, Paris, France
e-mail: guy.vasseur@upmc.fr

P. Rousseau-Gueutin
EHESP, Avenue du Professeur Léon-Bernard, F35043, Rennes, France

Introduction

In many parts of the world, especially where rainfall is scarce, surface water reserves (rivers, lakes or near-surface water bodies) are insufficient to satisfy human needs. Then, fresh groundwater resources from deep aquifers may offer an alternative supply. When these resources are exploited at a rate larger than their current recharge, their reserves will decrease more or less rapidly (Custodio 2002). Therefore, the understanding and quantification of processes associated with the recharge and discharge of these deep aquifers are essential for predicting and planning their exploitation (Scanlon et al. 2006).

The intensive exploitation of deep groundwater reserves is relatively recent (at most 50–100 years). Prior to human intervention, the recharge of groundwater systems had been modified by climate changes that occurred during the early Holocene or Pleistocene (Sonntag et al. 1980; Edmunds 2009). These changes in recharge conditions were particularly strong in arid and semi-arid areas of North-West to North-East Africa and in Eastern Australia. In the Sahara, the so-called "African Humid Period" (AHP) at the beginning of the Holocene was characterized by greater rainfall than currently. This is confirmed by many biological and archaeological observations and by isotopic records (Gasse 2000; Taylor et al. 2009; Lézine et al. 2011). The present intense aridity of the Sahara is interpreted as the result of a rapid hydrological change which occurred some 4,000 years ago (Kröpelin et al. 2008; Krinner et al. 2012). The same phenomenon was detected in East Australia (Love et al. 1994) indicating a possible worldwide trend.

Large variations in average rainfall (and therefore of recharge) induce modifications in the behaviour of deep groundwater systems but with a time lag as a consequence of the internal transient behaviour of such systems in response to changes of boundary conditions (Edmunds 1999). The quantification of this transient behaviour is fundamental in explaining or predicting the time required by the hydraulic system to adjust to the new boundary conditions. The aim of this study is to evaluate quantitatively the time constant that characterizes the duration of this transient state.

To this end, the modification of the relevant boundary conditions is assumed to be instantaneous. Prior to this

modification, the system is assumed to be at equilibrium. Once the modification has taken place, the hydrodynamic system evolves toward a new equilibrium. This evolution can generally be approximated by a functional dependence in time of the form $\exp(-t/\tau)$ where the time constant τ characterizes the transient duration.

The time constant τ is a function of the various physical parameters of the aquifer system. The simplest case is that of a one-dimensional (1-D) confined homogeneous aquifer where one end has a prescribed input flux due to recharge, and the other end is at a prescribed head. Initially the head presents a linear equilibrium profile. If at t=0, the prescribed flux becomes null, i.e. the recharge is suddenly set to 0, the system evolves toward a new equilibrium profile where everywhere the head equals the prescribed head at the output. The transient evolution of the hydraulic head may be computed analytically as a solution of the diffusion equation. It can be shown (Domenico and Schwartz 1998) that the time constant τ is given by:

$$\tau = \frac{4a^2}{\pi^2 D} \quad (1)$$

where a is the length of the aquifer and D its hydraulic diffusivity (ratio of its transmissivity T to its storage coefficient S).

This classical expression was generalized by Rousseau-Gueutin et al. (2013) to account for a more complex situation inspired by the structure of the Great Artesian Basin (GAB) in Australia. Their model is a one dimensional (1-D) mixed-aquifer system composed of two contiguous compartments. The upper compartment is an unconfined aquifer (subscript u), recharged by rainfall and with a relatively large storage coefficient. The discharge takes place at the end of the lower compartment which is a confined aquifer (subscript c) with the same transmissivity as the unconfined one. Starting from an assumed initial condition, the hydraulic head relaxes toward equilibrium in an (almost) exponential way. The time constant τ of this relaxation is a function of the geometrical properties (lengths a_u and a_c), storage coefficients (S_u and S_c) and transmissivity T (assumed to apply to both compartments). Moreover, for values of the storage parameters such that $a_u S_u$ is larger than $a_c S_c$, the parameter S_c has a negligible influence and the expression of the time constant reduces to:

$$\tau \approx \frac{a_u a_c S_u}{T} \quad (2)$$

This study aims to further discuss the conditions under which this formula or alternative ones can be used. The previous approach by Rousseau-Gueutin et al. (2013) is generalized by introducing alternative assumptions on the geometry (1-D along the horizontal direction, or cylindrical), or by using different values of hydraulic parameters and initial and boundary conditions.

Sonntag (1986) already developed similar arguments for interpreting the transient behaviour of the large Nubian Sandstone Aquifer (NSA) in North Africa. His study is based on the use of elementary harmonic solutions of the time-dependant diffusion equation for the head. Both linear 1-D cases and a cylindrical geometry (cylindrical mountain or depression) are considered. The present study differs from Sonntag's by the precise definition of initial conditions, by the use of a more realistic geometry and by the assumption of abrupt changes in recharge/discharge conditions allowing the use of Laplace transforms (Carslaw and Jaeger 1959).

In the present study, a generic model sketching the major features of some large aquifers of arid or semi-arid basins in North Africa and Australia is proposed. It is based on the observation of three geographic areas where large-scale characterization of aquifer behaviour are available: the North Western Sahara Aquifer System (NWSAS; Ould Baba Sy 2005; OSS 2003), the Nubian Sandstone Aquifer (NSA; Heinl and Brinkmann 1989), and the Great Artesian Basin in Australia (GAB; Rousseau-Gueutin et al. 2013). Using the same type of mathematical development, a set of models corresponding to various assumptions is proposed to describe the time evolution of the head in aquifers subjected to a sudden recharge variation. The time evolution of the head is obtained as a series of exponential terms decreasing with time. The first term of the series is strongly dominant which justifies the definition of a single time constant, expressed analytically as a function of a minimum number of parameters.

Formulation of a generic model: geometric and hydraulic parameters

The simplified generic model is based on reference examples of large aquifer basins with horizontal dimensions in the range 500–1,500 km such as NWSAS, NSA and GAB. A simplification of the structures described in the available monographs makes it possible to distinguish three zones in these large aquifer basins:

1. *A recharge zone* associated with the relief which generally bounds part of the basin. This relief receives (and has received in the past) a great amount of rainfall and generates high hydraulic heads in contiguous aquifers (Fig. 1a).
2. *A large deep aquifer* layer assimilated to a homogeneous and confined aquifer whose geometry can be greatly simplified (1-D in the horizontal direction or with a cylindrical symmetry).
3. *An outlet zone* where discharge occurs. This outlet may be either the sea or a surface-water body (lake, river, swamp) or a humid zone where evapotranspiration maintains a constant level.

DOI 10.1007/s10040-015-1252-3

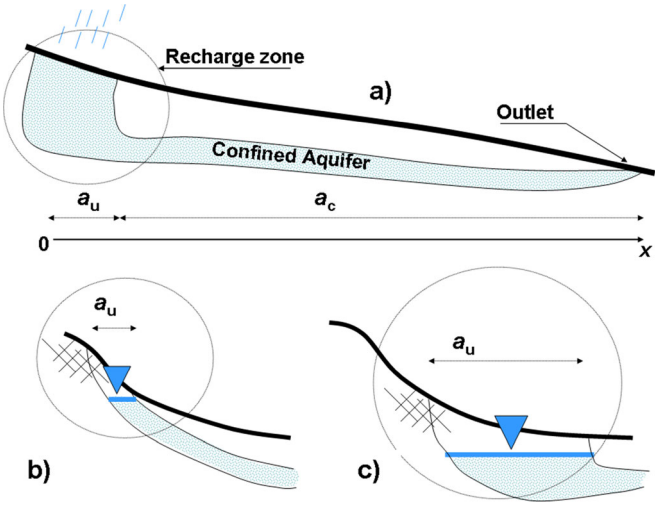

Fig. 1 Simplified scheme of the assumed 1-D aquifer system. **a** Schematic cross-section of a mixed aquifer: its upper part with width a_u is unconfined and receives the rainfall recharge, and its lower part with width a_c is confined down to the outlet. **b** Detail of the upstream recharge zone in the case where it corresponds to the surface outcrop of the aquifer. **c** Case where the upstream aquifer has a relatively wide dimension

In more detail:

1. The *recharge zone* of any of the referenced basins is actually part of their mountainous borders: the Atlas Mountain for the NWSAS, the Enedi for the NSA and the Great Dividing Range for the East GAB. In arid and semi-arid regions, these mountainous zones are considered as the water towers of neighbouring basins (Viviroli et al. 2003, 2007) due to orographic meteorological effects (Chavez et al. 1994; Wilson and Guam 2000).

   Infiltration of runoff water in the foothills, in particular during floods (Chavez et al. 1994), is the main recharge of deeper aquifers. The connexion may be local on the outcrops of the deep aquifers as illustrated in Fig. 1b where the outcrops of deep aquifers form several-km wide strips such as occurs in NWSAS on the southern side of the Atlas Mountain (Ould Baba Sy 2005). Alternatively, the deep aquifer can be recharged through a wide, superficial water-table aquifer with a large extent (50–300 km) beginning at the front of the mountain range. This case is illustrated in Fig. 1c and would apply to NSA and GAB.

   In any case, the recharge zone can be assimilated to an unconfined aquifer characterized by its geometry (width a_u), its hydraulic parameters (storage parameter S_u and transmissivity T_u) and its recharge rate (in fact the variation of this rate). For such an unconfined aquifer, the specific yield S_u (or effective porosity) is in the range of 10^{-2} – 10^{-1} for most porous or fractured sedimentary rocks. Conversely, the transmissivity T_u—defined as the product of the permeability by the saturated thickness—is poorly known and will be parameterized in the model.
2. *The large deep aquifers* which occupy most of North Africa and East Australia have a wide horizontal range (up to 1,500 km) and a considerable vertical thickness (several hundred m) ensuring their hydraulic continuity. In the NWSAS of Algeria, two such aquifers are well known: the "Continental Intercalaire confined aquifer (CI)" comprising formations from Middle Jurassic to Lower Cretaceous and the "Complexe Terminal (CT)" with Upper Cretaceous to Miocene formations (Ould Baba Sy 2005). Both aquifers are considered confined or semi-confined. In North East Africa, the aquifer system of NSA corresponds to Lower Cretaceous formations with a horizontal continuity over 500 km from the Ennedi and Tibesti mountains down to the Mediterranean Sea (Thorweilhe and Heinl 2002; Hesse et al. 1987) and it is confined in its northern part. In East Australia, the GAB, which occupies more than 20 % of the continent, is a multilayer aquifer where the flow runs mainly from the Great Dividing Range in a south-western direction through a more than 1,300-km wide area. It is confined over most of its extent (Rousseau-Gueutin et al. 2013).

   In the generic model, the deep aquifer is schematized by a confined aquifer with width a_c on the order of 500–1,500 km and homogeneous hydraulic properties: transmissivity T_c and storage coefficient S_c. Estimates of these parameters are available for the three basins under study. They are summarized in Table 1 and present quite a good consistency for the order of magnitude of T_c and S_c.
3. The *natural outlets* where these aquifers discharge are situated either in the sea or on the continental crust as springs or recharge of wadis (e.g. Oued Rhir in the NWSAS), surface-water bodies or chotts (i.e. playas) and swampy areas with low topography and a high evaporation rate (oases and humid areas with vegetation such as NSA).

   The model describes the natural evolution of the system, characterized by its specific time constant, when its recharge is submitted to external variations; therefore, artificial withdrawals for irrigated agriculture and domestic uses are not specifically taken into account. Moreover, a single outlet is assumed and corresponds to a condition of prescribed head.

   This simple geometry and the parameters defined in the preceding are the generic elements for computing the time constant. The basic model developed in the next section corresponds strictly to Fig. 1a. It consists of a mixed-aquifer system: its upper part is the recharge zone and its lower part is driving the flow toward the outlet. Then it is shown that, under certain conditions, it is possible to replace the recharge zone of this 1-D model by a boundary condition. Furthermore, the possible importance of horizontally convergent or divergent flow is studied in a following section, which describes discharge of a reservoir–aquifer system with cylindrical axial symmetry.

Time constant for the discharge of a 1-D mixed aquifer

The 1-D mixed aquifer model (Fig. 1a) has two components: the first one with width a_u is the recharge zone and

DOI 10.1007/s10040-015-1252-3

Table 1 Parameters characterizing the major confined aquifers of three basins

Basin name	a_c (km)	T_c (m^2s^{-1})	S_c	Reference
NSA	500	$6{\cdot}10^{-3}$	$2{\cdot}10^{-4}$–$3{\cdot}10^{-2}$	Heinl and Brinkmann 1989
NWSAS	1,000–2,000	10^{-3}–10^{-2}	10^{-4}–$2{\cdot}10^{-3}$	Sonntag 1999; OSS 2003 OSS 2003 Ould Baba Sy 2005
GAB	1,500	$5{\cdot}10^{-3}$–10^{-2}	$2{\cdot}10^{-4}$–$5{\cdot}10^{-3}$	Rousseau-Gueutin et al. 2013

the second one with width a_c is the deep aquifer driving the flow toward the outlet. Both aquifers are assumed homogeneous but they differ by the values of the hydraulic parameters (transmissivity, specific yield and storage coefficient). Before the initial time t=0, the head results from a stable equilibrium between an infiltration in the recharge zone and a discharge at the extremity of the deep aquifer. At time t=0, the recharge is modified (for example it reduces to 0) and a transient evolution toward a new equilibrium occurs. This is a generalization of the model developed by Rousseau-Gueutin et al. (2013) with the possibility of using different transmissivities and more realistic initial values.

Making use of the Dupuit's approximation (Marsily 1986), and assuming that in the unconfined aquifer at the recharge zone, variations of the saturated thickness can be neglected so that its transmissivity is constant, the hydraulic head $h(x,t)$ then satisfies a linear 1-D diffusion equation in both aquifers, with different hydraulic parameters. The previous study by Rousseau-Gueutin et al. (2013) using a numerical model to check the influence of a constant saturated thickness has shown that this approximation is satisfactory.

Here, contrary to Rousseau-Gueutin et al. (2013), the two components of the aquifer ($0<x<a_u$ and $a_u<x<a_u+a_c=a$) are characterized by their own transmissivities T_u,T_c; but, as proposed by these authors, they have their own storage coefficients S_u, S_c as well as their diffusivity coefficients $D_u=T_u/S_u$,$D_c=T_c/S_c$.$S_u>>S_c$ and the differences between the two components can be characterized by different ratios such as:

$$r = \sqrt{\frac{T_c S_c}{T_u S_u}} \tag{3}$$

$$f = \sqrt{\frac{T_u S_c}{T_c S_u}} = \sqrt{\frac{D_u}{D_c}} \tag{4}$$

from which:

$$rf = \frac{S_c}{S_u} \text{ and } \frac{r}{f} = \frac{T_c}{T_u} \tag{5}$$

The boundary conditions are that the head is null at the outlet and that upstream of the recharge zone, at x=0, the flux is null ($\partial h/\partial x$=0). Moreover, at the limit between the two aquifers ($x=a_u$), the head is continuous as well as the hydraulic flux. Therefore:

$$\begin{aligned} &T_u \frac{\partial h}{\partial x}(0,t) = 0 \\ &h(a,t) = 0 \\ &h^-(a_u,t) = h^+(a_u,t) \\ &T_u \frac{\partial h^-}{\partial x}(a_u,t) = T_c \frac{\partial h^+}{\partial x}(a_u,t) \end{aligned} \tag{6}$$

where the superscripted symbols −/+ are relative to aquifers u/c.

Initially ($t\leq 0$), the head is at equilibrium under recharge to the upper aquifer and discharge occurs at $x=a$. Let B be the recharge rate for $0<x<a_u$. The equilibrium equations for the head write:

$$T_u \frac{\partial^2 h}{\partial x^2} + B = 0 \quad \text{for} \quad 0 < x < a_u \tag{7}$$

$$T_c \frac{\partial^2 h}{\partial x^2} = 0 \quad \text{for} \quad a_u < x < a_u + a_c \tag{8}$$

The solution which satisfies the boundary conditions (Eq. 6) is:

$$h^0(x) = B\left(\frac{a_u^2 - x^2}{2T_u} + \frac{a_u a_c}{T_c}\right) \quad \text{for} \quad 0 < x < a_u \tag{9}$$

$$h^0(x) = B a_u \frac{a - x}{T_c} \quad \text{for} \quad a_u < x < a_u + a_c \tag{10}$$

When at time t=0, the recharge suddenly stops, the system tends toward a new equilibrium where $h(x,+\infty)$=0. This evolution is described by a diffusion equation assuming B=0 and the same boundary conditions (Eq. 6). The time-dependant hydraulic head then satisfies for $t>0$:

$$S_u \frac{\partial h}{\partial t} = T_u \frac{\partial^2 h}{\partial x^2} \quad \text{for} \quad 0 < x < a_u \tag{11}$$

$$S_c \frac{\partial h}{\partial t} = T_c \frac{\partial^2 h}{\partial x^2} \quad \text{for} \quad a_u < x < a_u + a_c \tag{12}$$

with the boundary conditions (Eq. 6) and the initial conditions (Eqs. 9–10).

DOI 10.1007/s10040-015-1252-3

As proposed by Carslaw and Jaeger (1959), it is useful to replace this problem by a "complementary" one where the solution, called g(x,t), has an initial condition g(x,0)=0 everywhere. g(x,t) is assumed to obey the same boundary conditions (Eq. 6) but now, for t>0, it is subjected to a recharge B for 0<x<a_u. The equations for this complementary problem write:

$$S_u\frac{\partial g}{\partial t} = T_u\frac{\partial^2 g}{\partial x^2} + B \qquad \text{for } 0 < x < a_u \tag{13}$$

$$S_c\frac{\partial g}{\partial t} = T_c\frac{\partial^2 g}{\partial x^2} \qquad \text{for } a_u < x < a_u + a_c \tag{14}$$

It is easy to show that the initial head $h(x,t)$ is related to $g(x,t)$ by:

$$h(x,t) = h^0(x) - g(x,t) \tag{15}$$

This stratagem based on linearity and homogeneity of both equations and boundary conditions, allows a much easier solution. Moreover, it can be used to compute the evolution of the potential for any sudden change of recharge conditions. Assume that at t=0 the recharge suddenly changes from B to B', then the transient solution for the hydraulic head $h(x,t)$ can be expressed as a function of the solution $g(x,t)$ of Eqs. (11–12) by:

$$h(x,t) = h^0(x) + g(x,t)\frac{B' - B}{B} \tag{16}$$

The mathematical solution of the "complementary" $g(x,t)$ is developed in Appendix 1. Taking into account Eq. (15), the full solution of the initial problem is expressed as:

$$h(x,t) = \frac{2B}{S_u D_c}\sum_{n=1}^{\infty}\frac{r\sin(\beta_n a_u/f)\cos(\beta_n x/f)\exp\left(-\beta_n^2 D_c t\right)}{\beta_n^3[a_c + a_u r/f + a_c(r^2-1)\cos^2(\beta_n a_u/f)]}$$
$$\text{for } 0 < x < a_u \tag{17}$$

$$h(x,t) = \frac{2B}{S_u D_c}\sum_{n=1}^{\infty}\frac{\cos(\beta_n a_u)\sin(\beta_n(a-x))\exp\left(-\beta_n^2 D_c t\right)}{\beta_n^3[a_c + a_u/rf + a_u(r^2-1)\cos^2(\beta_n a_c)/rf]}$$
$$\text{for } a_u < x < a \tag{18}$$

In these expressions, β_n is the nth real and positive root of the equation:

$$\Delta(\beta) = r\cos(a_c\beta)\cos(a_u\beta/f) - \sin(a_c\beta)\sin(a_u\beta/f) = 0 \tag{19}$$

Therefore the hydraulic head $h(x,t)$ is expressed as a series of exponential functions of time such as $\sum R_n(x)\exp(-t/\tau_n)$ where τ_n is given by $\tau_n = 1/(D_c\beta_n^2)$. For a given time t, the successive terms $R_n(x)\exp(-t/\tau_n)$ of this series rapidly decrease with n. In practice, the series can be reduced to its first term $R_1(x)\exp(-t/\tau_1)$. This simplification is quantitatively justified as illustrated in Fig. 2a which compares, for several truncations, the profile of the head, once normalized to its initial value at x=a_u, i.e. from Eqs. (9–10) normalized by $a_u a_c B/T_c$. For several values of t (t=0, t=τ_1, $2\tau_1$) and several ratios of the hydraulic parameters, the first term of the series is compared to more complete series (up to order n=5). From Fig. 2a, it is justified to retain only the first term: this is verified for the case T_u=T_c and will be later confirmed for more general cases. Therefore the full solution $h(x,t)$ given by Eqs. (17–18) can be replaced by:

$$h(x,t) \approx \frac{2B}{S_u D_c}\frac{r\sin(\beta_1 a_u/f)\cos(\beta_1 x/f)\exp\left(-\beta_1^2 D_c t\right)}{\beta_1^3[a_c + a_u r/f + a_c(r^2-1)\cos^2(\beta_1 a_u/f)]}$$
$$\text{for } 0 < x < a_u \tag{20}$$

$$h(x,t) \approx \frac{2B}{S_u D_c}\frac{\cos(\beta_1 a_u)\sin(\beta_1(a-x))\exp\left(-\beta_1^2 D_c t\right)}{\beta_1^3[a_c + a_u/rf + a_u(r^2-1)\cos^2(\beta_1 a_c)/rf]}$$
$$\text{for } a_u < x < a \tag{21}$$

Within the limits of this simplification, Eqs. (20–21) describe the exponential decrease with time of the head as $\exp(-t/\tau_1)$ with a time constant $\tau_1 = 1/D_c\beta_1^2$. As stated in the previous, the value of β_1 is the first positive root of Eq. (19) but it can be given an approximate analytical expression based on a limited development of $\Delta(\beta)$ in the vicinity of β=0. A second-order Taylor series development in β of Eq. (19) yields the first root of $\Delta(\beta)$=0 as:

$$\beta_1^2 \cong \frac{r}{\left[a_u a_c/f + r\left(a_u^2/f^2 + a_c^2\right)/2\right]} = \frac{1}{S_u/S_c\left[a_u a_c + (T_c/T_u)a_u^2/2\right] + a_c^2/2} \tag{22}$$

and the corresponding time constant:

$$\tau_1 = \frac{1}{D_c\beta_1^2} \cong \frac{a_c a_u S_u}{T_c} + \frac{a_u^2}{2D_u} + \frac{a_c^2}{2D_c} \tag{23}$$

This expression is similar to that given by Rousseau-Gueutin et al. (2013) with differences related to the fact that here $T_u \neq T_c$. The time constant τ_1 given by Eq. (23) is expressed as a sum of three terms which have different values depending on the geometric and hydraulic parameters. The two last terms of Eq. (23) reflect the contribution by the unconfined (subscripts u) and the confined part

DOI 10.1007/s10040-015-1252-3

(subscript c), respectively. The first term of Eq. (23) is a cross-contribution by u and c and will be shown to be the dominant contribution for the cases of interest.

The relative importance of the three terms in Eq. (23) can be assessed as shown in Table 3 (Appendix 1) which compares the relative contributions by the three terms of Eq. (23) for a wide range of aquifer parameters. It appears that, for S_c/S_u in the range 10^{-4} – 10^{-2}, the last term of Eq. (23) is relatively negligible (less than 5 % of the sum) for any T_c/T_u or a_u/a_c. Moreover, when $T_c \leq T_u$, the first term of Eq. (23) is clearly dominant (above 80 % of the sum). It should be noted that for $T_c=T_u$ and $S_c<<S_u$ the time constant Eq. (23) reduces to $\tau_1 \sim (S_u / T_c)\, a_u (a_c+a_u/2)$ which is exactly the formula proposed by Rousseau-Gueutin et al. (2013); however, a new aspect demonstrated by the present work is that the conductivity ratio T_c/T_u appears as a relatively important parameter, as illustrated in Fig. 2b,c.

The effect of this transmissivity difference can be assessed as follows: when $T_c/T_u<1$, the hydraulic head along the unconfined aquifer ($0<x<a_u$) as illustrated by Fig. 2b is almost constant. In other words, for $T_c<T_u$, the unconfined aquifer is playing the role of reservoir with a hydraulic head that is constant with x and which is feeding the neighbouring confined aquifer. Conversely, when $T_c/T_u>1$, as illustrated in Fig. 2c, the hydraulic head in the unconfined aquifer presents, near the position $x=a_u$, a strong gradient due to the low transmissivity of the neighbouring confined aquifer.

The unconfined aquifer is assumed to model the relatively elevated margins of the main confined aquifer and its actual hydraulic transmissivity is difficult to assess (Chavez et al. 1994; Viviroli et al. 2003, 2007). Nevertheless, it seems plausible that this recharge zone has a transmissivity at least equal to that of the deeper confined aquifer, i.e. that $T_u \geq T_c$. If this is the case, the unconfined aquifer can be modelled as a simple reservoir as developed in the next section.

From the mixed 1-D model to the discharge of a reservoir–aquifer system

As illustrated in Fig. 3, this 1-D model is obtained from the previous one in the case of very large T_u. Then, lateral variations of the head $h(x,t)$ in the unconfined aquifer can be neglected and the upper aquifer is reduced to a reservoir, or tank, of width a_u and storage capacity S_u connected to the lower confined aquifer. A single parameter $M=S_u a_u$ now characterises the integrated storage capacity of the reservoir. For $t<0$, the recharge still occurs for $0<x<a_u$ so that the hydraulic head of the reservoir is the same as that of the neighbouring confined reservoir at $x=a_u$. This is accounted for by the boundary condition at $x=a_u$: the flux entering the confined aquifer is equal to the rate at which the water mass inside the tank decreases, i.e. $Mh=S_u a_u h$. Mathematically, this is a boundary condition of the third type (or Fourier condition) prescribed at $x=a_u$ as a linear relation between the time derivative of $h(x,t)$ for $t>0$ and its space derivative:

$$M\frac{\partial h(a_u,t)}{\partial t} = T_c \frac{\partial h(x,t)}{\partial x}\bigg|_{x=a_u} \tag{24}$$

Before the initial time $t=0$, the assumed hydraulic head in the system results from an equilibrium between the recharge at rate B in the tank (for $0<x<a_u$) and the discharge at the end of the confined aquifer, at $x=a_u+a_c$. In the confined aquifer, the initial head varies linearly from $h=h_1$ at $x=a_u$ to $h=0$ at $x=a_u+a_c$ and the value $h(a_u,0)=h_1$ is related to the initial recharge rate B by:

$$h_1 = \frac{B a_c a_u}{T_c} \tag{25}$$

At $t=0$, the recharge suddenly stops and the tank feeds the confined aquifer until it is completely depleted. The evolution of the head toward a new equilibrium is obtained as the solution of the diffusion equation using Laplace transforms as explained in Appendix 2. This solution for $h(x,t)$ is shown to be:

$$h(x,t) = 2h_1 \sum_{n=1}^{\infty} \frac{\sin(\beta_n(a-x))\exp\left(-D_c\beta_n^2 t\right)}{a_c^2\beta_n^2 \sin(\beta_n a_c)\left[1+M/S_c a_c + (M\beta_n/S_c)^2\right]} \tag{26}$$

where β_n is the nth positive root of the equation in β:

$$\Delta(\beta) = \cos(\beta a_c) - (\beta a_c)\frac{M}{S_c a_c}\sin(\beta a_c) = 0 \tag{27}$$

As in the previous case, the first term ($n=1$) of the series Eq. (26) is highly dominant so that this series can be truncated to yield:

$$h(x,t) \cong 2h_1 \frac{\sin[\beta_1(a-x)]\exp\left(-D_c\beta_1^2 t\right)}{a_c^2\beta_1^2 \sin(\beta_1 a_c)\left[1+M/S_c a_c + (M\beta_1/S_c)^2\right]} \tag{28}$$

which describes the exponential decrease of $h(x,t)$. Furthermore, a linear development of $\Delta(\beta)$ in the vicinity of $\beta=0$ shows that the first root β_1 of Eq. (27) can be approximated by:

$$\beta_1 \cong \frac{1}{a_c\sqrt{[1/2 + M/(S_c a_c)]}} \tag{29}$$

As shown in Table 4 of Appendix 2, this approximation appears to be satisfactory to within 5 % as long as $M/(S_c a_c)>1$.

DOI 10.1007/s10040-015-1252-3

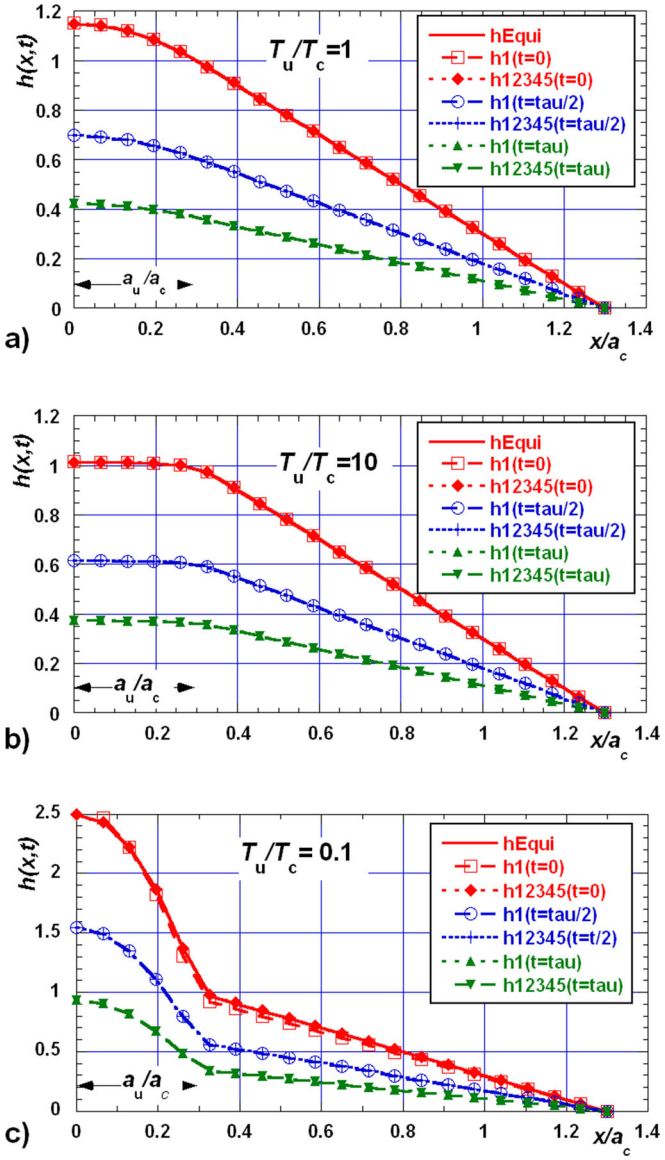

Fig. 2 Evolution of the hydraulic head for unconfined-confined aquifers with a_u=0.3, a_c=1 (a_c+a_u=1.3), a ratio of specific storage $S_u/S_c=10^2$ and three ratios of transmissivity: **a** T_u/T_c =1, **b** T_u/T_c =10, and **c** T_u/T_c =0.1. The various curves correspond to three values of time (0,τ/2, τ) and to various approximations. The head is initially at equilibrium between its recharge for 0<x<0.3 a_c and discharge at x=a_c+a_u. The three curves labelled *hEqu*, *h1(t=0)* and *h12345(t=0)* correspond to the true value and to two approximations for the initial head using either the first root β_1 or the five first ones. The curves labelled *h1(tau/2)* and *h12345(tau/2)* illustrate two approximations for $h(x,\tau/2)$, and those labelled *h1(tau)* and *h12345(tau)* the corresponding approximations for $h(x,\tau)$. In most cases, the various approximations are practically indistinguishable.

According to these results, for any x, the head $h(t)$ decreases exponentially toward 0 as $\exp(-t/\tau)$ where the time constant τ is:

$$\tau = \frac{1}{D_c\beta_1^2} \cong \frac{a_c^2}{D_c}\left[1/2 + M/(S_c a_c)\right] = \frac{a_c^2}{2D_c} + \frac{a_c a_u S_u}{T_c} \quad (30)$$

On the basis of this formula, it is interesting to discuss the implication of the various hydraulic parameters on the order

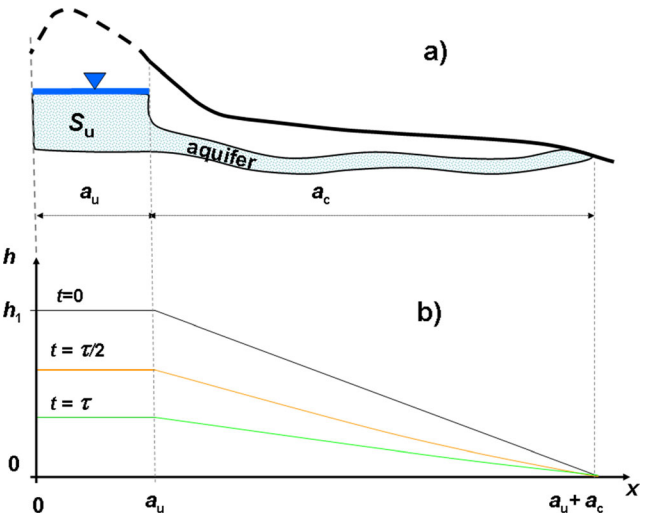

Fig. 3 Reservoir/confined-aquifer system. **a** Schematic cross-section of the system. The confined aquifer with width a_c stands for a_u<x<a_c+a_u. The outlet is at x=a_c+a_u and the limit x=a_u is connected to a reservoir with width a_u and storage S_u . **b** Corresponding evolution of the hydraulic head in the reservoir and in the confined aquifer.

of magnitude of the time constant τ. When the integrated storage M=$S_u a_u$ of the upper unconfined aquifer is negligible compared to that of the confined one ($S_c a_c$) then $\tau \approx a_c^2/2D_c$. This is consistent to within 20 % with the exact solution for an isolated confined layer given in Eq. (1). When using parameters relevant to this confined aquifer (T_c~10^2 m^{2}s^{-1}, S_c~10^4 implying D_c~10^2 m^{2}s^{-1} and a_c ~500 km), one obtains τ~40 years which is a very low value.

Compared to this basic configuration of an isolated confined aquifer, the storage capacity due to the unconfined aquifer drastically increases the estimated value of τ as implied by the second term of Eq. (30). In fact, the case where $S_u a_u >> S_c a_c$ is quite realistic, since S_u is on the order of 0.1 which greatly exceeds S_c ~10^{-4}. Assuming a_u~100 km and a_c~500 km results in $M/S_c a_c$ ~200 and a value of τ on the order of 15,000 years. This is well above the estimate neglecting the unconfined storage. With such assumptions, Eq. (30) reduces to:

$$\tau \cong \frac{a_c M}{T_c} = \frac{a_c a_u S_u}{T_c} \quad (31)$$

which is similar to Eq. (2).

2-D effects: discharge of a reservoir–aquifer system with cylindrical symmetry

In the two previous sections, a 1-D model was assumed, which implies that, on average, the velocity vector is everywhere parallel to x. The present section deals with two-dimensional (2-D) effects due to converging or diverging flow prescribed by the basin geometry. For this study, the reservoir–aquifer system of Fig. 3 is extended

DOI 10.1007/s10040-015-1252-3

by rotation around a vertical axis. With respect to Fig. 3, this vertical axis is fixed either at $x<0$ in order to study a divergent flow or at $x>a_c+a_u$ for the convergent one. Such geometries are quite similar to those proposed by Sonntag (1986) for the study of NSA (his models of a cylindrical mountain or cylindrical depression).

Diverging flow: model of an "island" or "cylindrical mountain"

This model requires a radial coordinate r which measures the distance with respect to the vertical axis of symmetry (at $r=0$). A topographic height (or "island") surrounds the axis. The central area $0<r<R$, or part of it, serves as a reservoir where the recharge takes place by precipitation, seepage, etc. This central reservoir is loading a radially diverging confined aquifer which occupies the area: $R<r<R+a_c$. The outlet of the aquifer is at $r=R+a_c$. The model is represented on Fig. 4. Of course, the model does not need to be fully cylindrical; a "slice" of the cylinder, like a slice of pizza, is sufficient.

The unconfined aquifer, where rainfall contributes to the recharge, is located along a circular zone defined by $R-a_u<r<R$. Its specific yield is S_u and its width along the radial distance is a_u with a_u ranging from 0 to R. For $a_u=0$, the reservoir comprises the whole circle $r<R$ and the surface-integrated water reserve is given by $S_u\pi R^2$. The specific case considered here assumes $a_u<<R$ so that the reservoir forms a ring of small width a_u with an integrated water surface reserve given by $S_u 2\pi Ra_u$ or a volume reserve $S_u 2\pi Rha_u$.

The reservoir is connected to the external confined aquifer beginning at $r=R$. The decrease rate of the reservoir volume compensates the input flux into the surrounding aquifer. The boundary condition at $r=R$ in the confined aquifer is a linear relation between the time derivative of the head and its normal derivative at $r=R$:

$$2\pi RS_u a_u \frac{\partial h(R,t)}{\partial t} = 2\pi RT_c \frac{\partial h(r,t)}{\partial r}\bigg|\, r=R$$

or, with $M=S_u a_u$:

$$M\frac{\partial h(R,t)}{\partial t} = T_c \frac{\partial h(r,t)}{\partial r}\bigg|\, r=R \tag{32}$$

(The case of a reservoir using the whole surface $r<R$ may be dealt with by defining M as $S_uR/2$ instead of S_ua_u). The other boundary condition corresponds to the outlet (fixed head) prescribed at $r=R+a_c$; therefore, $h(R+a_c,t)=0$.

The confined aquifer in the area $R<r<R+a_c$ is characterized by T_c (its transmissivity) and S_c (its storage coefficient), whence $D_c=T_c/S_c$ is its diffusivity. Since the flow is radial, the hydraulic head $h(r,t)$ satisfies the diffusion equation in cylindrical coordinates.

$$\frac{T_c}{r}\frac{\partial}{\partial r}\left(r\frac{\partial h}{\partial r}\right) = S_c\frac{\partial h}{\partial t} \tag{33}$$

The initial hydraulic head of the confined aquifer is the result of an equilibrium between the prescribed recharge condition Eq. (32) at $r=R$ and its discharge at $r=R+a_c$ prescribing $h=0$. The general solution of the steady-state cylindrical equation (i.e. corresponding to Eq. (33) with

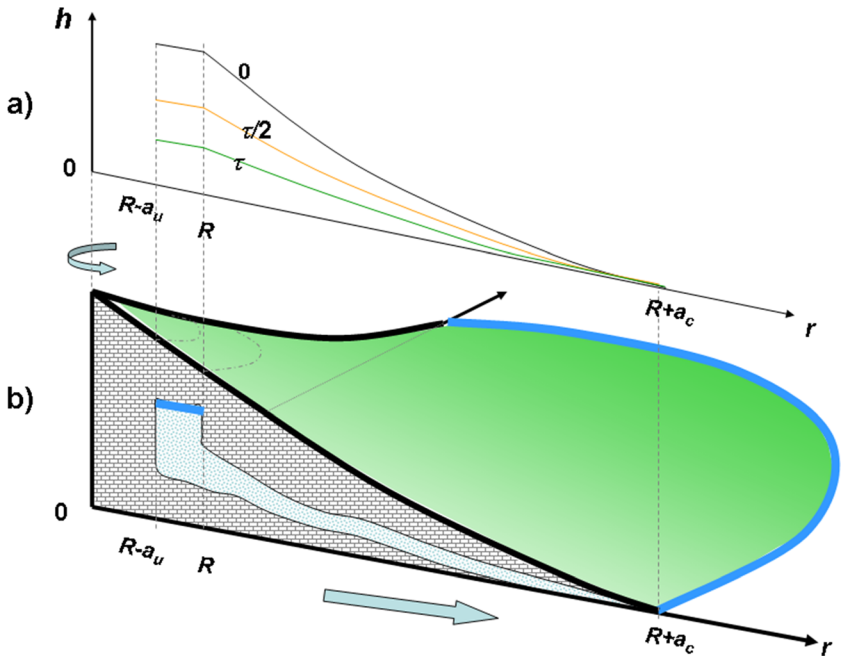

Fig. 4 Schematic cross-section and 3-D view of the model used for a divergent flow. **a** The evolution of the head in the aquifer along a radial direction or from the initial condition when recharge was occurring in the reservoir for $R-a_u<r<R$. **b** A perspective view of the symmetrical model with divergent flow (from $r=0$). The outlet is at $r=R+a_c$

 DOI 10.1007/s10040-015-1252-3

$\partial h/\partial t=0$) which satisfies $h(R)=h_1$ and $h(R+a_c)=0$ is now logarithmic in r and can be written:

$$h(r) = h_1 \frac{\ln(R+a_c)-\ln(r)}{\ln(R+a_c)-\ln(R)} \tag{34}$$

The constant h_1 (the initial head) is a function of the rainfall-seepage rate B:

$$h_1 = B\frac{a_u R}{T_c}\ln\left(\frac{R+a_c}{R}\right) \tag{35}$$

From this initial solution, the transient evolution can now be calculated as a solution of Eq. (33) using the same techniques. This solution is developed in Appendix 3 as:

$$h(r,t) = h_1 \sum\nolimits_{n=1}^{\infty} \exp\left(-D_c\beta_n^2 t\right) k_n(r) \tag{36}$$

where $k_n(r)$ is a function depending on Bessel functions J_0, J_1, Y_0, and Y_1, and β_n is the nth positive root of the equation in β:

$$\begin{aligned}&\{J_0[\beta_n R]Y_0[\beta_n(R+a_c)]-J_0[\beta_n(R+a_c)]Y_0[\beta_n R]\}+\\&\{J_0[\beta_n(R+a_c)]Y_1[\beta_n R]-J_1[\beta_n R]Y_0[\beta_n(R+a_c)]\}=0\end{aligned} \tag{37}$$

The first root β_1 of this equation is approximated by expanding it when β is in the vicinity of 0. This yields:

$$\beta_1 \cong \frac{1}{\sqrt{R^2\left[\left(\frac{M}{S_c R}-\frac{1}{2}\right)\ln\left(\frac{R+a_c}{R}\right)+\frac{(R+a_c)^2-R^2}{4R^2}\right]}} \tag{38}$$

and the corresponding time constant:

$$\tau = \frac{1}{D_c\beta_1^2} \cong \frac{a_c^2}{D_c}\left\{\frac{1+2R/a_c}{4}-(R/a_c)^2\left(\frac{1}{2}-\frac{M}{S_c R}\right)\ln(1+a_c/R)\right\} \tag{39}$$

When $a_c<<R$, the cylindrical geometry approaches that of a 1-D case. In this case, the expression of τ given by Eq. (39) may be expanded as a function of a_c/R:

$$\tau \to \tau_{lim} \cong \frac{a_c^2}{D_c}\left[\frac{1-a_c/3R}{2}+\frac{M}{S_c a_c}(1-a_c/2R)\right] \tag{40}$$

This expression is quite similar to Eq. (30) which applies to the 1-D model; the difference is that the first term is multiplied by $(1-a_c/3R)$ and the second one by $(1-a_c/2R)$. Compared to the model of parallel flow in the previous section, the divergent nature of the flow results in a decrease of the time constant τ as can be expected intuitively.

The limiting case where $M>>S_c R$ deserves attention. When the upstream storage of water is dominant, Eq. (39) reduces to:

$$\tau \cong \ln\left(\frac{\rho}{R}\right)\frac{S_u a_u R}{T_c}+\frac{\rho^2-R^2}{4D_c} \tag{41}$$

where $\rho=R+a_c$ is the radius of the outlet. Moreover, if ρ/R is large enough so that $\ln(\rho/R)$ is at least on the order of 1, Eq. (41) becomes:

$$\tau \cong \ln\left(\frac{\rho}{R}\right)\frac{S_u a_u R}{T_c} = \ln\left(\frac{R+a_c}{R}\right)\frac{S_u a_u R}{T_c} \tag{42}$$

The latter expression presents some analogy with the corresponding asymptotic one (Eq. 30) valid for the 1-D case: Eq. (42) involves R instead of a_c for Eq. (31) but τ decreases when a_c/R increases.

Converging flux: model of a "lake" or "cylindrical depression"

This is the convergent version of the axially symmetric model. In this case, the recharge margins with high topography are located at $r=R$ along the external limits of the basin, whereas the outlet lies closer to its centre at $r=\rho=R-a_c$, (with $a_c<R$). Between these two structures, for $R-a_c<r<R$, a convergent flow occurs in the main confined aquifer, with transmissivity T_c and storage coefficient S_c over a width a_c as shown in Fig. 5. The reservoir associated with the recharge zone is a narrow ($a_u<<R$) circular fringe ($R<r<R+a_u$) which is hydraulically connected to the main confined aquifer. The integrated storage capacity of this reservoir is characterized by the parameter $M=S_u a_u$.

In the aquifer, the head satisfies a diffusion equation similar to Eq. (33), the difference being the boundary conditions. The prescribed conditions at the reservoir–aquifer limit arise from the assumptions of head continuity and conservation of mass, which yields, at $r=R$:

$$M\frac{\partial h(R,t)}{\partial t} = -T_c\frac{\partial h(r,t)}{\partial r}\bigg|\, r=R \tag{43}$$

At the outlet, the boundary condition is $h(R-a_c,t)=0$. (Note that the assumption $a_c=R$ would be misleading because for such convergent flow, the hydraulic head at $r=0$ would be undefined). The general solution of the steady-state cylindrical equation (i.e. corresponding to Eq. (33) with $\partial h/\partial t=0$) which satisfies $h(R)=h_1$ and $h(R-a_c)=0$, is:

$$h(r) = h_1(r)\frac{\ln(R-a_c)-\ln(r)}{\ln(R-a_c)-\ln(R)} \tag{44}$$

DOI 10.1007/s10040-015-1252-3

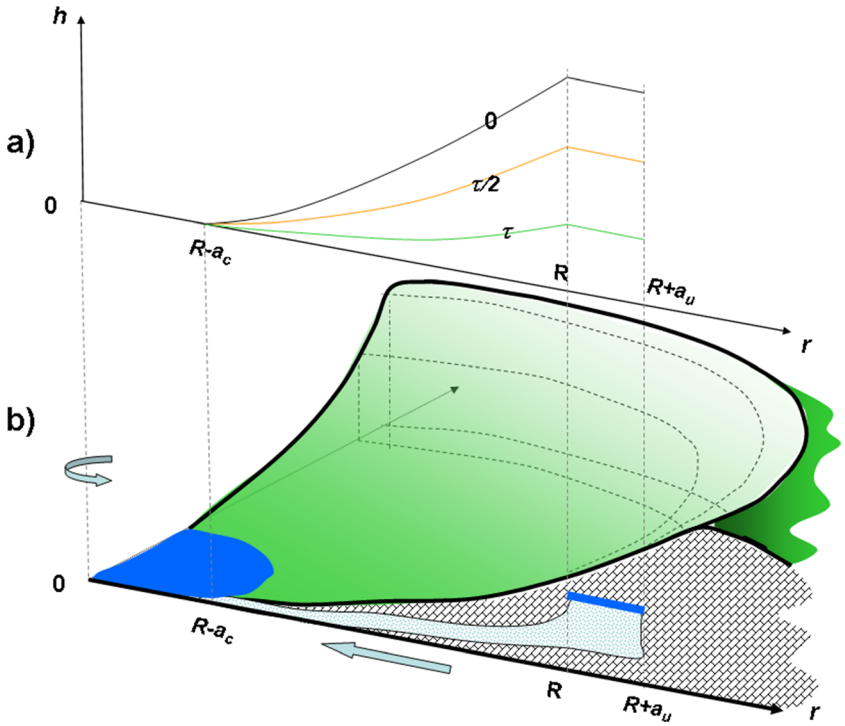

Fig. 5 Schematic cross-section and three-dimensional (3-D) view of the model used for a convergent flow. **a** The evolution with time of the head in the aquifer along a radial direction, from the initial condition when recharge was occurring in the reservoir. **b** A perspective view of the symmetrical model of convergent flow (toward r=0). The outlet is at $r=R-a_c$ and the reservoir lies within $R<r<R+a_u$

and h_1 can be expressed as a function of the recharge rate and hydraulic parameters:

$$h_1 = B\frac{a_u R}{T_c}\ln\left(\frac{R}{R-a_c}\right) \tag{45}$$

Starting from this initial solution, the transient evolution is calculated as a solution of Eq. (33) as developed in Appendix 3 and yields:

$$h(r,t) = h_0\sum\nolimits_{n=1}^{\infty}\exp\left(-D_c\beta_n^2 t\right)kk_n(r) \tag{46}$$

where $kk_n(r)$ is also a function depending on Bessel functions J_0, J_1,Y_0, and Y_1, and β_n is the nth positive root of the equation in β:

$$\Delta(\beta) = \{-J_0[\beta_n R]Y_0[\beta_n(R-a_c)] + J_0[\beta_n(R-a_c)]Y_0[\beta_n R]\} + \{J_0[\beta_n(R-a_c)]Y_1[\beta_n R] - J_1[\beta_n R]Y_0[\beta_n(R-a_c)]\} = 0 \tag{47}$$

As previously, the first root β_1 of this equation may be approximated by:

$$\beta_1 \cong \frac{1}{\sqrt{R^2\left[\left(\frac{M}{S_c R}+\frac{1}{2}\right)\ln\left(\frac{R}{R-a_c}\right)+\frac{(R-a_c)^2-R^2}{4R^2}\right]}} \tag{48}$$

corresponding to a time constant:

$$\tau = \frac{1}{D_c\beta_1^2} \cong \frac{a_c^2}{D_c}\left\{\frac{1-2R/a_c}{4} - (R/a_c)^2\left(\frac{1}{2}+\frac{M}{S_c R}\right)\ln(1-a_c/R)\right\} \tag{49}$$

For $a_c<<R$, the expression of τ obtained by expanding Eq. (49) as a function of a_c/R approaches that of the 1-D case:

$$\tau \to \tau_{\lim} \cong \frac{a_c^2}{D_c}\left[\frac{1+a_c/3R}{2}+\frac{M}{S_c a_c}(1+a_c/2R)\right] \tag{50}$$

With respect to the 1-D model, the first term of τ is multiplied by $(1+a_c/3R)$ and the second term by $(1+a_c/2R)$. Therefore, the convergent flow is associated with an increase of the time constant τ as has already been suggested.

In the case where $M>>S_c R$, Eq. (49) reduces to:

$$\tau \cong \ln\left(\frac{R}{\rho}\right)\frac{S_u a_u R}{T_c} + \frac{\rho^2-R^2}{4D_c} \tag{51}$$

where $\rho=R-a_c$ is the radius of the outlet ($\rho<R$). Moreover, if R/ρ is large enough so that $\ln(R/\rho)$ is at least of the order of 1, Eq. (51) becomes:

$$\tau \cong \ln\left(\frac{R}{\rho}\right)\frac{S_u a_u R}{T_c} = \ln\left(\frac{R}{R-a_c}\right)\frac{S_u a_u R}{T_c} \tag{52}$$

which is analogous to Eq. (42) in the case of divergent flow. However, in this case, the logarithmic factor

DOI 10.1007/s10040-015-1252-3

becomes very large when a_c tends toward R, i.e. when the radius of the outlet becomes negligible.

Conclusion on convergence–divergence effects

The whole set of results concerning the effects of divergence/convergence on the time constant is summarized in Fig. 6, where the time constants τ obtained for various models of flow (diverging, parallel and converging) are presented. The ordinate is the time constant τ normalized to the basic parameter D_c/a_c^2 and the abscissa is the ratio a_c/R which characterizes the curvature of the system. The various curves correspond to various values of the normalized storage capacity $M/(S_c a_c)$. The abscissa $a_c/R=0$ corresponds to the 1-D model, with parallel flow, the abscissa $a_c/R>0$ to a diverging flow and, by convention, the abscissa $a_c/R<0$ to a converging flow. In the latter case, the parameter a_c/R ranges from 0 (no convergence) to −1; the last value corresponds to the limit where $a_c \rightarrow |R|$ so that the head has a singular behaviour. Figure 6 confirms that the flow divergence induces a decrease of τ as a function of the curvature, which is unlimited since a_c/R is not limited. However, the convergence results in a very significant increase of τ, which may even be very large when the size of the outlet tends toward 0. For a small curvature (a_c/R close to 0), the slope of the normalized τ as a function of $|a_c/R|$ follows the previously predicted trends with a slope of −1/3 for low $M/S_c a_c$ and −1/2 for large $M/S_c a_c$.

Discussion and application

The obtained formulas are now applied to actual transient phenomena occurring in the selected basins.

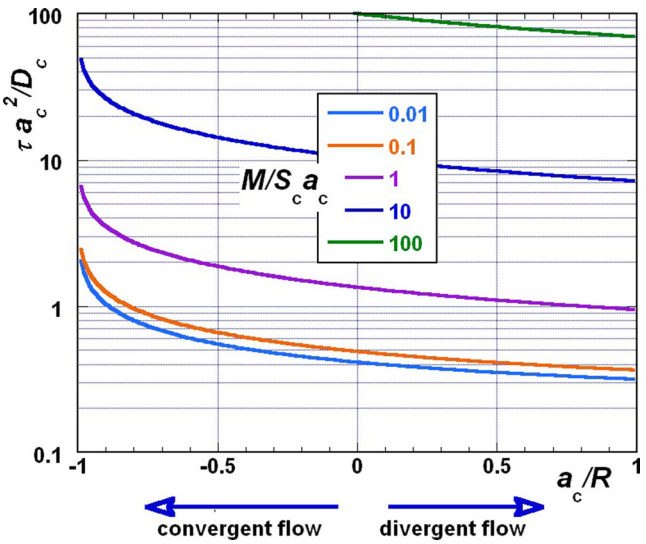

Fig. 6 Chart of the normalized correction applied to the time constant in the divergent and convergent cases. The curves show the reduced value of τ (normalized by a_c^2/D_c) as a function of the curvature of the reservoir zone, characterized by a_c/R: by convention $a_c/R<0$ is a convergent flux. The curves are parameterized by the normalized storage of the reservoir $M/S_c a_c$

Since the presented models are based on many simplifications, only first-order phenomena are considered, with particular attention to the hydraulic parameters and the large-scale geometry of the systems.

The large aquifer basins of North Africa and East Australia received, during the early Holocene, abundant rainfall which stopped around 4,000 years BP resulting in the present arid climate (Gasse 2000; Taylor et al. 2009; Lézine et al. 2011). This drastic decrease in rainfall and recharge for a period of 4,000 years and the recent withdrawals of groundwater for agricultural use are clearly responsible for the critical piezometric falls observed in some deep aquifers (e.g. Besbes and Horriche 2007 for the NWSAS). However, these observations are hardly significant at the regional scale. In fact, local drawdowns of piezometric levels observed in areas of intense withdrawal are clearly associated with local pumping effects: their apparent time constant τ (defined as $\tau=h/(\partial h/\partial t)$, i.e. assuming an exponential decay of $h(t)$) is on the order of 100 years. This is much smaller than the time constant associated with recharge variations.

If one assumes that no rainfall has recharged these deep aquifers for about 4,000 years, the fact that they are not completely depleted indicates that their time constant τ is on the order of several thousand years. Alternatively, it has been proposed that some modern rainfall-recharge is still occurring even though it is much weaker than it was at the beginning of the Holocene (Ould Baba Sy 2005; Gonçalvez et al. 2013). In any case, the time constant defined in the present study is still valid since it represents a sudden modification of the recharge rate, no matter if the final state tends toward a complete drought. In this case, τ would characterize the evolution from an initial "very rainy" situation to a "less rainy" one.

As stated in the definition of the generic model, the confined aquifers of the large basins NWSAS, NSA and GAB are characterized by the following parameters: $T_c \sim 10^3$–10^2 $m^2 s^{-1}$, $S_c \sim 10^4$ and a_c ~500 km. Assuming that these confined aquifers are not connected to any unconfined aquifer operating as a reservoir, then from Eq. (1), their time constant τ would be in the range 40–400 years, i.e. much less than the 4,000 years of the beginning of dry conditions. Therefore, without modern recharge, these aquifers would be depleted.

As noted previously, the value of τ drastically increases when the main confined aquifer is connected to an upstream unconfined one with a much larger storage capacity. According to Eq. (30), valid for $T_u \geq T_c$, the presence of an unconfined layer characterized by $S_u a_u = 5\ S_c a_c$ is sufficient to multiply the previous τ value by a factor of about 11. This factor can easily be obtained: assuming $S_c \sim 10^4$ and $a_c \sim 500$ km, even a narrow reservoir with $a_u \sim 2.5$ km and $S_u \sim 10^1$ would be sufficient.

Therefore, the *presence of an upstream unconfined aquifer* coupled with the recharge zone plays a major role *for maintaining the head in the whole basin* during

DOI 10.1007/s10040-015-1252-3

periods on the order of 1–10 ka. In the cases of NSA (Heinl and Brinkmann 1989) and GAB (Habermehl 1980), relatively large unconfined aquifers with widths in the range 50–200 km, connected to the main confined one, have been observed. For NWSAS, the CI and CT main aquifers present many outcrops at the periphery of the basin (such as the Atlas Mountain range) with widths on the order of a few tens of km (Ould Baba Sy 2005). These narrow outcrops may behave as potential reservoirs where recharge occurred in the past and still continues.

Another important geometrical factor resulting in a larger τ value is *the convergence of hydraulic flows* which affects many basins, as shown by present piezometric maps. In the CI aquifer of NWSAS groundwater flows converge on the Gulf of Gabes in South Tunisia (Besbes and Horriche 2007). In Australia, a concentration of groundwater flows toward Lake Eyre occurs in the endorheic GAB basin (Habermehl 1980). The confined aquifer of NSA also presents converging features toward the Gulf of Syrte (Heinl and Brinkmann 1989). Such convergent geometry can be modelled by the cylindrical model for converging flow (Fig. 5). Assume that the discharge zone which represents the outlet has a radius of 100 km; if the main aquifer has a width a_c=500 km, the radius where the recharge zone is active becomes R=600 km. This leads to a ratio a_c/R=− 0.8 to –0.9, with a minus sign according to the convention used in Fig. 6. For such a ratio, a convergence-induced multiplicative factor of around 3–4 applies to τ, as can be seen in Fig. 6. This significantly contributes to the durability of the system. Therefore, the evaluation of the time constant of large aquifer basins suggests that their geometry and structure explain why they are still discharging water when they have been subjected to arid conditions for more than 4,000 years. Moreover, this evaluation is not modified by the possible contribution of a small modern rainfall recharge.

The concept of time constant can also be applied to a previous transient phenomenon: the onset of the "green Sahara". At the beginning of the Holocene, the currently arid Sahara was much wetter than today (Gasse 2000; Taylor et al. 2009; Lézine et al. 2011). From about 12,500 to 6,000 years BP, its lowlands contained many freshwater bodies now almost completely dried out (this wet phase was followed by the current dry period which occurred around 4,000 years BP). During this humid event, a time-lag on the order of 3,000 years has been shown to have existed between the onset of the wet period and the maximum development of freshwater bodies. The chronology is based on the interpretation of many palaeohydrology observations at the scale of the whole Sahara (Lézine et al. 2011) and of high-quality data in specific areas such as Lake Yoa in Northern Chad (Grenier et al. 2009). A likely explanation is that this time-lag reflects the delayed contribution of groundwater to the near-surface-water bodies, i.e. the time necessary for the recharge of deep aquifers (starting at the onset of the humid period) to reach the outlets. The time constant computed here for application to the discharge of large Saharan basins may also be applied to their recharge. A time-lag of several thousand years between the onset of the humid period and their maximum extent is indeed consistent with the estimated time constant.

This study can be used to give a first-order estimate of the natural decay time of the hydraulic head. In many instances, unconfined aquifers provide a major contribution to water reserves and can be assimilated to reservoirs. A quite robust Eq. (31) was obtained for the case where the unconfined reservoir-like aquifer has an integrated storage capacity M=$S_u a_u$ much larger than $S_c a_c$: the time constant τ reduces to $\tau \sim M\ a_c/T_c = S_u a_u a_c/T_c$, which does not depend any more on S_c and T_u. Realistic evaluations of a_c, a_u and T_c are often available and S_u is related to the local porosity (another possibility is to make use of existing remote gravity measurements that record variations of the water mass over time (e.g. GRACE), as proposed by Sun et al. (2010).

For the previous applications, relatively large values of τ are explained by the major role of unconfined aquifers with storage coefficients much larger than those of confined ones. This feature has already been emphasized by many authors (e.g. OSS 2005, which is a report for the NWSAS) and deserves further discussion. The value of S_u can generally be estimated as the accessible porosity, which is generally on the order of 0.1 (Marsily 1986). By contrast, the low storage coefficient S_c of confined aquifers is due to the compressibility of the water and of the pore volume and depends mainly on the mechanical deformation ability of rocks. The resulting S_c value lies in the range 1/100–1/1000 of that of S_u; however, the existence of such a great difference of storativity suggests several limitations. First, during a depletion event, the top of the confined aquifer may become unsaturated in some places so that its behaviour becomes that of an unconfined one. Second, possible vertical fluxes (leakage) between neighbouring aquifers have been neglected, whereas they may contribute to increase the available water storage. For instance, Bredehoeft et al. (1983) found that leakage due to fractures is important in explaining the head distribution in the confined Dakota Aquifer System (USA). In fact, Eq. (30) applies to a case where the confined aquifer is hydraulically isolated from its surroundings except through the connection with its upstream unconfined neighbour.

Equation (31) may also receive a very simple physical interpretation: the time constant τ is similar to that of a falling head permeameter for measuring the "hydraulic resistance" a_c/T_c of a porous medium limiting the discharge toward an outlet (Marsily 1986). This analogy was already used by Ould Baba Sy (2005) to reconstruct the "initial" hydraulic head of the NWSAS aquifers at the beginning of the dry period.

Conclusions

This work is a continuation of the previous study by Rousseau-Gueutin et al. (2013) of the transient depletion

DOI 10.1007/s10040-015-1252-3

of a mixed (unconfined-confined) aquifer system when subjected to a sudden recharge change. The various models developed here present both a generalization of the previous study for more complex and more realistic cases (initial condition, 2-D effects, etc.), and some simplifications where the initial water storage is geometrically concentrated.

When such a mixed aquifer system is submitted to an abrupt change of recharge, the hydraulic head evolution from an initial equilibrium to a final one closely follows an exponential trend $\exp(-t/\tau)$ characterized by the time constant τ. For simple geometries, τ is expressed analytically as a function of the characteristics of the system: the hydraulic parameters (transmissivities T_u,T_c and storage coefficients S_u, S_c) and the geometrical ones (width of the two components a_u, a_c and for the cylindrical case, radius R of the recharge zone). Table 2 summarizes the analytical formulae expressing τ as a function of these parameters as developed in the previous analytical sections. These formulae are labelled from Nos. 1 to 10; each of them corresponds to a specific assumption made on the values of the parameters as well as on the actual geometry of the flow pattern. Since these various formulae are to be used in practical situations, the following paragraphs are providing some guidance for discussing their relevance domain.

Formulae Nos. 1–4 apply to the linear 1-D case where the curvature of the flow lines can be neglected, whereas formulae Nos. 5–10 emphasize the role of cylindrical flow characterised by the curvature radius R of the upstream reservoir.

For the linear 1-D case, formula No. 1 applies to the general case of a mixed aquifer and does not need any specific assumption. However, in practice, several approximations are often justified since the upstream aquifer component of the basic model is identified as an unconfined aquifer with large storage capacity ($S_c << S_u$). In fact, the relevant formula also depends on the relative values of transmissivities: the case where $T_c=T_u$ leads to formula No. 2 (already developed by Rousseau-Gueutin et al. 2013); if $T_u >> T_c$, it is possible to replace the upstream component of width a_u and large capacity S_u by an equivalent reservoir of integrated storage a_uS_u resulting in formula No. 3. If, moreover, the horizontally integrated a_uS_u is much larger that a_cS_c, then formula No. 3 reduces to No. 4 where the parameters S_c and T_u are absent.

The effects of radial convergence or divergence are to be discussed on the basis of cylindrical models; only the case where $T_u >> T_c$ is considered where the upstream component can be replaced by an equivalent reservoir with curvature radius R. Formulae Nos. 5 and 7 respectively give the expression of τ for the general case of a diverging flow or a converging one; these formulae are the counterparts of formula No. 3 in the case of cylindrical symmetry. The effect of a weak curvature ($a_c<<R$) is assessed by formulae Nos. 6 and 9 through comparison with formula No. 3 based on the linear model: the marginal effect of divergence (No. 6) or convergence (No. 9) is characterized by the factor$\pm a_c/R$. When, moreover, the horizontally integrated a_uS_u is much larger than a_cS_c, the effect of an important curvature (i.e. a_c on the order of R) results in formula No. 7 (for divergence) and No. 10 (for convergence).

It is important to notice that, in many commonly occurring conditions, the analytical expression of τ depends on only four parameters that characterize the system: the width a_c of the main confined aquifer, its transmissivity T_c, the integrated storage situated upstream $M=S_ua_u$ and the curvature R of the reservoir describing the convergence/divergence of the flow. These ultra-simplified expressions are given in Table 2 as Nos. 3, 7 and 10.

These expressions were applied to several large aquifer basins of the Sahara and Australia. Following the sudden occurrence of the present aridity around 4,000 years ago, these deep confined aquifers have been subjected to a natural head decay with a large time constant (τ>5,000 years) resulting from their structure and geometry. This large time constant τ can be explained by the existence of an upstream water reserve in the form of an unconfined aquifer. The convergence of groundwater flow also results

Table 2 Summary of analytical expressions obtained

Formula N°	Geometry	Assumption on parameters	Expression of the time constant τ
1	1D Mix. Aquif.[a]	No assumption	$a_ua_c(S_u/T_c)+a_u^2S_u/(2T_u)+a_c^2S_c/(2T_c)$
2	1D Mix. Aquif.	$T_u=T_c$; $S_c<< S_u$	$a_u(a_c+a_u/2)S_u/T_c$
3	1D Res. Aquif.[b]	$T_u>>T_c$	$a_ca_uS_u/T_c+a_c^2S_c/(2T_c)$
4	1D Res. Aquif.	$T_u>>T_c$; $a_uS_u >>a_cS_c$	$a_ca_uS_u/T_c$
5	2D Cyl. Div.[c]	$T_u>>T_c$	$a_c^2S_c/T_c\{ (1+2R/a_c)/4-(R/a_c)^2[1/2-a_uS_u/(S_cR) \ln(1+a_c/R)\}$
6	2D Cyl. Div.	$T_u>>T_c$; $a_c<<R$	$a_c^2S_c/T_c[(1+a_c/3R)/2+ (1+a_c/2R)(a_uS_u)/(a_cS_c)]$
7	2D Cyl. Div.	$T_u>>T_c$; $a_c\#^e R$; $a_uS_u>>a_cS_c$[e]	$Ra_uS_u/T_c\{\ln[(R+a_c)/R]\}$
8	2D Cyl. Conv.[d]	$T_u>>T_c$	$a_c^2S_c/T_c\{(1-2R/a_c)/4-(R/a_c)^2[1/2+a_uS_u/(S_cR)] \ln(1-a_c/R)\}$
9	2D Cyl. Conv.	$T_u>>T_c$; $a_c<<R$	$a_c^2/D_c[(1-a_c/3R)/2+ (1-a_c/2R) (a_uS_u)/(S_ca_c)]$
10	2D Cyl. Conv.	$T_u>>T_c$; $a_c\#R$; $a_uS_u>>a_cS_c$	$Ra_uS_u/T_c\{\ln[R/(R-a_c)]\}$

[a] Corresponds to linear mixed aquifer system

[b] Corresponds to linear reservoir–aquifer system

[c] Corresponds to axial symmetry with divergent flow

[d] Corresponds to axial symmetry with convergent flow

[e] # corresponds to of the same order of magnitude

 DOI 10.1007/s10040-015-1252-3

in a significantly enhanced time constant τ. Both effects have contributed to the natural persistence of flow at the outlet of these aquifers for 4,000 years. The same mechanisms may also have been responsible for the apparent time delay observed in the Sahara between the onset of a climatic wet phase at the beginning of the Holocene and the maximum extent of the humid zones.

Acknowledgements The authors gratefully acknowledge discussions with A.M. Lézine, C. Leduc and P. Genthon. We also thank C. Grenier and C. Simmons for fruitful remarks and Mrs G. de Marsily for linguistic improvement.

Appendices

Appendix 1: Laplace transform solution for the 1-D mixed aquifer system

The auxiliary function $g(x,t)$ defined in the text is satisfying:

$$S_u\frac{\partial g}{\partial t} = T_u\frac{\partial^2 g}{\partial x^2} + B \quad \text{for } 0 < x < a_u \tag{53}$$

$$S_c\frac{\partial g}{\partial t} = T_c\frac{\partial^2 g}{\partial x^2} \quad \text{for } a_u < x < a_u + a_c = a \tag{54}$$

Its initial condition is that $g(x,0)=0$ for any x in the range $(0, a=a_u+a_c)$. Its boundary conditions are:

$$\begin{aligned} &T_c\frac{\partial g}{\partial x}(0,t) = 0 \\ &g(a,t) = 0 \\ &g^-(a_u,t) = g^+(a_u,t) \\ &T_u\frac{\partial g^-}{\partial x}(a_u,t) = T_u\frac{\partial g^+}{\partial x}(a_u,t) \end{aligned} \tag{55}$$

Let $\gamma(x,p)$ be the Laplace transform of $g(x,t)$; $\gamma(x,p)$ satisfies:

$$S_u p\gamma = T_u\frac{\partial^2 \gamma}{\partial x^2} + \frac{B}{p} \quad \text{for } 0 < x < a_u \tag{56}$$

$$S_c p\gamma = T_c\frac{\partial^2 \gamma}{\partial x^2} \quad \text{for } a_u < x < a_u + a \tag{57}$$

with boundary conditions similar to those of $g(x,t)$ as Eq. (55). When introducing the parameter q defined by:

$$q = \sqrt{\frac{pS_c}{T_c}} = \sqrt{\frac{p}{D_c}} \tag{58}$$

the general solution of Eq. (56) can be written as:

$$\gamma(x,p) = \frac{B}{p^2 S_u} + \alpha\cosh\left(\frac{qx}{f}\right) + \delta\sinh\left(\frac{qx}{f}\right) \quad \text{for } 0 < x < a_u \tag{59}$$

and that of Eq. (57) as:

$$\gamma(x,p) = \lambda\cosh(qx) + \xi\sinh(qx) \quad \text{for } a_u < x < a_u + a_c \tag{60}$$

The four constants a,δ,λ,ξ are obtained by the four boundary conditions (Eq. 55) and the solution is:

$$\gamma(x,p) = \frac{B}{p^2 S_u}\left[1 - r\frac{\cosh(a_c q)\cosh(qx/f)}{\Delta}\right] \quad \text{for } 0 < x < a_u \tag{61}$$

$$\gamma(x,p) = \frac{B}{p^2 S_u}\left[\frac{\sinh(a_u q/f)\cosh[q(a-x)]}{\Delta}\right] \quad \text{for } a_u < x < a = a_u + a_c \tag{62}$$

where Δ is the determinant defined by:

$$\Delta = r\cosh(a_c q)\cosh(a_u q/f) + \sinh(a_c q)\sinh(a_u q/f) \tag{63}$$

For taking the inverse Laplace transform, it is necessary to identify the singularities of $\gamma(x,p)$ in the complex p plane. The function $\gamma(x,p)$ is single valued. It has a simple pole at $p=0$ and an infinite series of simple poles p_n on the negative part of the real axis.

The pole at $p=0$ corresponds to the asymptotic trend of the solution for $t\to+\infty$. Its expression is obtained as the limit of Eqs. (61)–(62) for $p\to 0$:

$$\gamma(x,p\to 0) \approx \frac{B}{p}\left(\frac{a_u^2 - x^2}{2T_u} + \frac{a_u a_c}{T_c}\right) \quad \text{for } 0 < x < a_u \tag{64}$$

$$\gamma(x,p\to 0) \approx \frac{B}{p}a_u\frac{a-x}{T_c} \quad \text{for } a_u < x < a_u + a_c \tag{65}$$

This asymptotic behaviour corresponds to the steady-state solution $g(x,t\to+\infty)$. From the definition of $g(x,t)=h^0(x)-h(x,t)$, $g(x,+\infty)$ is also equal to the assumed initial value $h^0(x)$, the expression of which (Eqs. 9–10) can be recognized in Eqs. (64)–(65) to within a $1/p$ multiplicative factor.

The other poles correspond to the p_n values where $\Delta(p_n)=0$. Using Eq. (58), these poles in p correspond to purely imaginary values of $q_n = \sqrt{p_n/D_c} = i\beta_n$ where β_n is real. Using a trigonometric transformation of Eq. (63), the poles are also the zeros in β of the function $\Delta\beta$:

$$\Delta(\beta) = r\cos(a_c\beta)\cos(a_u\beta/f) - \sin(a_c\beta)\sin(a_u\beta/f) = 0 \tag{66}$$

 DOI 10.1007/s10040-015-1252-3

The first and smallest zero of Eq. (66) can be approximated from a first-order expansion of $\Delta\beta$) in the vicinity of β=0:

$$\Delta(\beta) \approx r - \beta^2 \left[\frac{r}{2} \left(\frac{a_u^2}{f} + a_c^2 \right) + \frac{a_u a_c}{f} \right] \tag{67}$$

This first root β_1 of $\Delta\beta$=0 can be approximated by:

$$\beta_1 \approx \sqrt{\frac{r}{a_u a_c/f + r(a_u^2/f + a_c^2)/2}} = \frac{1}{\sqrt{a_u a_c \frac{S_u}{S_c} + a_u^2 \frac{T_c S_u}{2 T_u S_c} + \frac{a_c^2}{2}}} \tag{68}$$

The inverse transform is obtained through integration in the complex p plane as (Carslaw and Jaeger 1959):

$$g(x,t) = \frac{1}{2i\pi} \int_c \gamma(x,p) \exp(pt) dp \tag{69}$$

The contour C of the integral lies parallel to the imaginary axis, from $-\infty$ to$+\infty$, and is closed in such a way that all singularities of the function (p) are located in the left part of the complex p-plane. It is closed on a large circle in the left part of the p-plane, which gives a vanishing contribution. This contour integral allows the use of the residuals theorem and each pole gives a contribution to the integral Eq. (69) according to the behaviour of $\gamma(x,p)$. The pole at p=0 contributes to give the asymptotic function $h^0(x)$. The other poles p_n associated with the β_n (n=1,2…) solutions of $\Delta\beta$=0 contribute to give a function $R_n(x)\exp(-tD_c/{\beta_n}^2)$. Here $R_n(x)$ denotes the residual, i.e. the linear trend of the function $\gamma(x,p)$ in the vicinity of the pole $p_n=-{\beta_n}^2 D_c$. This yields:

$$g(x,t) = B\left(\frac{a_u^2 - x^2}{2T_u} + \frac{a_u a_c}{T_c} \right) - \frac{2B}{S_u D_c} \sum_{n=1}^{\infty} \frac{r \sin(\beta_n a_u/f) \cos(\beta_n x/f) \exp\left(-\beta_n^2 D_c t\right)}{\beta_n^3 [a_c + a_u r/f + a_c (r^2-1) \cos^2(\beta_n a_u/f)]} \tag{70}$$

for $0<x<a_u$ and

$$g(x,t) = B a_u \frac{a-x}{T_c} - \frac{2B}{S_u D_c} \sum_{n=1}^{\infty} \frac{\cos(\beta_n a_u) \sin(\beta_n (a-x)) \exp\left(-\beta_n^2 D_c t\right)}{\beta_n^3 [a_c + a_u/rf + a_u (r^2-1) \cos^2(\beta_n a_c)/rf]} \tag{71}$$

for $a_u<x<a_u+a_c$.

Using Eq. (15), the expression of $h(x,t)$ is found directly from that of $g(x,t)$ as $h(x,t)=h^0(x) - g(x,t)$ yielding the results (Eqs. 17–18).

In practice, as explained in the main text, the summation over n (1… ∞) can generally be restricted to the first term n=1 since the other terms (n=2,3…) give a negligible contribution. The time variation closely follows an exponential decrease $h(x,t)\propto\exp(-{\beta_1}^2 D_c t)$ or $h(x,t)\propto\exp(-t/\tau)$ where τ is the time constant. From Eq. (68), this time constant may be approximated by:

$$\tau \approx \frac{1}{\beta_1^2 D_c} \approx a_u a_c \frac{S_u}{D_c S_c} + a_u^2 \frac{T_c S_u}{2 D_c T_u S_c} + a_c^2 \frac{1}{2 D_c} = a_u a_c \frac{S_u}{T_c} + a_u^2 \frac{S_u}{2 T_u} + a_c^2 \frac{S_c}{2 T_c} \tag{72}$$

The relative importance of the three terms in Eq. (72) can be assessed as shown in Table 3 which gives in percent the relative contributions by these three terms for a wide range of aquifer parameters. Three parameter ratios (of storage coefficients, horizontal widths and transmissivities) have a range of variation inspired by the considered aquifer basins:

- The storage coefficient S_c/S_u ratio is in the range 10^{-4} – 10^{-1} for characterizing the difference in storage between confined and unconfined aquifers.
- The horizontal width a_u/a_c ratio between the two types of aquifers is assumed to vary between 0.1 (localized recharge zone) and 0.5 (wide recharge zone).
- The transmissivity T_c/T_u ratio is largely arbitrary. It is assumed to vary in the range 10^{-1} – 10^{1}.

It is clear that, for S_c/S_u in the range 10^{-4}– 10^{-2}, the last term of Eq. (72) is relatively negligible (less than 5 % of the sum) for any T_c/T_u or a_u/a_c and that when $T_c \le T_u$, the first term of Eq. (72) is clearly dominant (above 80 % of the sum), which results in further simplification of Eq. (72) as discussed in the main text.

Appendix 2: Laplace transform solution for the 1-D reservoir–aquifer system

The head $h(x,t)$ satisfies the diffusion equation:

$$S_c \frac{\partial h}{\partial t} = T_c \frac{\partial^2 h}{\partial x^2} \quad \text{for } a_u < x < a_u + a_c = a \tag{73}$$

with the two boundary conditions:

$$h(a_u + a_c = a, t) = 0 \tag{74}$$

$$M \frac{\partial h(a_u, t)}{\partial t} = T_c \frac{\partial h(x,t)}{\partial x}\bigg|_{x=a_u} \tag{75}$$

DOI 10.1007/s10040-015-1252-3

Table 3 Relative value in % of the three terms of Eq. (72) vs. values of ratios $S_c/S_u T_c/T_u$, a_u/a_c

T_c/T_u	a_u/a_c	S_c/S_u=0.0001 relative value in %			S_c/S_u=0.001 relative value in %			S_c/S_u=0.01 relative value in %			S_c/S_u=0.1 relative value in %		
0.1	0.1	99.45	0.50	0.05	99.01	0.50	0.50	94.79	0.47	4.74	66.45	0.33	33.22
0.1	0.2	98.99	0.99	0.02	98.77	0.99	0.25	96.62	0.97	2.42	79.37	0.79	19.84
0.1	0.5	97.55	2.44	0.01	97.47	2.44	0.10	96.62	2.42	0.97	88.89	2.22	8.89
1	0.1	95.19	4.76	0.05	94.79	4.74	0.47	90.91	4.55	4.55	64.52	3.23	32.26
1	0.2	90.89	9.09	0.02	90.70	9.07	0.23	88.89	8.89	2.22	74.07	7.41	18.52
1	0.5	79.99	20.00	0.01	79.94	19.98	0.08	79.37	19.84	0.79	74.07	18.52	7.41
10	0.1	66.64	33.32	0S.03	66.45	33.22	0.33	64.52	32.26	3.23	50.00	25.00	25.00
10	0.2	49.99	49.99	0.01	49.94	49.94	0.12	49.38	49.38	1.23	44.44	44.44	11.11
10	0.5	28.57	71.43	0.00	28.56	71.41	0.03	28.49	71.23	0.28	27.78	69.44	2.78

The first boundary condition is that the head is 0 at the outlet $x=a$. The second boundary condition means that the aquifer is connected to a reservoir which has the same head $h(a_u,t)$ at $x=a_u$ as the aquifer. This reservoir is characterized by its integrated storage capacity $M=a_u S_u$. The reservoir–aquifer connection implies that any time variation of the reservoir volume induces a diffusive flux toward (or from) the aquifer at $x=a_u$.

The initial condition is that, at $t=0$, the system is at equilibrium between a discharge at $x=a$ and a recharge of the reservoir at a rate B per unit coordinate for $0<x<a_u$. This yields the following linear solution of the equilibrium equation in the aquifer:

$$h(x,0) = h_1 \frac{a-x}{a_c} \quad \text{for } a_u < x < a \tag{76}$$

where h_1 is such that the flux of water $T_c h_1/a_c$ entering in the aquifer compensates the integrated recharge Ba_u. Therefore:

$$h_1 = B\frac{a_c a_u}{T_c} \tag{77}$$

Let $\eta(x,p)$ be the Laplace transform of the function $h(x,t)$; the associated equation for $\eta(x,p)$ is:

$$S_c\left[p\eta - h_1\frac{a-x}{a_c}\right] = T_c\frac{\partial^2\eta}{\partial x^2} \quad \text{for } a_u < x < a_u + a_c \tag{78}$$

Introducing $q = \sqrt{p/D_c}$ the general solution of Eq. (78) is:

$$\eta(x,p) = \frac{h_1}{p}\frac{a-x}{a_c} + \alpha\cosh(qx) + \delta\sinh(qx) \tag{79}$$

with two constants α and δ which are determined to satisfy Eqs. (74)–(75). This gives:

$$\eta(x,p) = \frac{h_1}{p}\left\{\frac{a-x}{a_c} - \frac{T_c\sinh(q(a-x))}{qa_c[T_c\cosh(qa_c) + MD_c q\sinh(qa_c)]}\right\} \tag{80}$$

Again, the function $\eta(x,p)$ is single valued and has an infinite series of simple poles p_n on the negative part of the real axis. The value $p=0$ is not a pole, as can be verified with a limited development of Eq. (80) for small p. The poles are the zeros of the expression at the denominator of Eq. (80) and can also be expressed as functions of the real variable $\beta = -iq = \sqrt{-p/D_c}$. The corresponding β values are positive solutions of:

$$\begin{aligned}\Delta(\beta) &= T_c\cosh(qa_c) + MD_c q\sinh(qa_c)\\ &= T_c\cos(\beta a_c) - MD_c\beta\sin(\beta a_c) = 0\end{aligned} \tag{81}$$

The Laplace inversion proceeds as for Appendix 1. The poles p_n corresponding to the positive β_n (n=1,2…) solutions of $\Delta(\beta)=0$ contribute to the contour integral (as defined in Eq. 69). This contribution is a function $R_n(x)\exp(-tD_c/\beta_n{}^2)$ where $R_n(x)$ denotes the residual, i.e. the linear trend of the function $\eta(x,p)$ in the vicinity of the pole $p_n = -\beta_n^2/D_c$. The expression for the residual is:

$$R_n(x) = 2h_1\frac{\sin[\beta_n(a-x)]}{a_c^2\beta_n^2\sin(\beta_n a_c)\left[1 + M/S_c a_c + (M\beta_n/S_c)^2\right]} \tag{82}$$

and the required solution is an infinite series:

$$h(x,t) = 2h_1\sum_{n=1}^{\infty}\frac{\sin[\beta_n(a-x)]\exp\left(-tD_c/\beta_n^2\right)}{a_c^2\beta_n^2\sin(\beta_n a_c)\left[1 + M/S_c a_c + (M\beta_n/S_c)^2\right]} \tag{83}$$

In practice, the summation over n (1… ∞) is restricted to the first term n=1 since the other terms (n=2,3…) give a negligible contribution. The time variation closely follows an exponential decrease $h(x,t)\propto\exp(-\beta_1{}^2 D_c t)$ or $h(x,t)\propto\exp(-t/\tau)$ where τ is the time constant $\tau = 1/\beta_1{}^2 D_c$. An approximate value

DOI 10.1007/s10040-015-1252-3

of β_1 is obtained from a first-order expansion of $\Delta(\beta)$ given by Eq. (82) in the vicinity of β=0:

$$\beta_1 \cong \frac{1}{a_c\sqrt{[1/2 + M/(S_c a_c)]}} \tag{84}$$

Table 4 allows a comparison between the approximate Eq. (84) and the exact value of β_1 obtained by a numerical solution of Eq. (81). The approximation (Eq. 84) appears to be satisfactory to within 5 % as long as $M/(S_c a_c)>1$.

Therefore the time constant $\tau=1/{\beta_1}^2 D_c$ may be approximated by:

$$\tau = \frac{1}{D_c\beta_1^2} \cong \frac{a_c^2}{D_c}\left[\frac{1}{2} + \frac{M}{S_c a_c}\right] = \frac{a_c^2}{2D_c} + \frac{a_c a_u S_u}{T_c} \tag{85}$$

Appendix 3: Laplace transform solution for the cylindrical reservoir–aquifer system with divergent or convergent flow

In radial coordinates, the head is assumed to depend only on the radius r and to satisfy the corresponding radial diffusion equation for $h(r,t)$:

$$\frac{T_c}{r}\frac{\partial}{\partial r}\left(r\frac{\partial h}{\partial r}\right) = S_c\frac{\partial h}{\partial t} \tag{86}$$

For the case of *diverging flow*, the domain of the aquifer is $R<r<R+a_c$. A boundary condition is prescribed at the outlet $r=R+a_c$ as $h(R+a_c)=0$. The other condition at $r=R$ is a connection with a reservoir with integrated storage given by $M=a_u S_u$. This implies a mixed boundary condition on the value of h at $r=R$:

$$M\frac{\partial h(R,t)}{\partial t} = T_c\frac{\partial h(r,t)}{\partial r}\bigg|\, r = R \tag{87}$$

Table 4 Comparison of exact numerical values of $(\beta_1 a_c)$ and approximation (Eq. 84)

$M/S_c a_c$	$(\beta_1 a_c)$ Exact numerical value	$(\beta_1 a_c)$ Approximated by Eq. (84)
100	0.0998	0.0997
10	0.3111	0.3086
1	0.8603	0.8165
0.1	1.4288	1.2910
0.0	Π/2	√2

The general solution of the steady-state equation which satisfies $h(R+a_c)=0$ is:

$$h(r) = h_1\frac{\ln(R+a_c)-\ln(r)}{\ln(R+a_c)-\ln(R)} \tag{88}$$

h_1 can be expressed as a function of the initial recharge rate B. For $t\le 0$, the water budget requirement is that the flow entering the aquifer is equal to the integrated recharge. Therefore:

$$h_1 = B\frac{a_u R}{T_c}\ln\left(\frac{R+a_c}{R}\right) = B\frac{MR}{T_c S_u}\ln\left(\frac{R+a_c}{R}\right) \tag{89}$$

Let $\eta(r,p)$ be the Laplace transform of the function $h(r,t)$; its associated equation is:

$$S_c\left[p\eta - h_1\frac{\ln[(R+a_c)/r]}{\ln[(R+a_c)/R]}\right] = \frac{T_c}{r}\frac{\partial}{\partial r}\left(r\frac{\partial\eta}{\partial r}\right) \tag{90}$$

$$\text{for } R < r < R + a_c$$

Using $q=\sqrt{p/D_c}$, the general solution of Eq. (90) is obtained as a function of the modified Bessel functions I_0 and K_0:

$$\eta(x,p) = \frac{h_1}{p}\frac{\ln[(R+a_c)/r]}{\ln[(R+a_c)/R]} + \alpha I_0(qr) + \delta K_0(qr) \tag{91}$$

α and δ are defined to satisfy the boundary conditions. This leads to:

$$\eta(x,p) = \frac{h_1}{pR\ln[(R+a_c)/R]}\left\{R\ln\left[\frac{R+a_c}{r}\right] + \frac{\kappa\left[-I_0(qr)K_0[q(R+a_c)] + I_0[q(R+a_c)]K_0(qr)\right]}{p\left[I_0(qR)K_0[q(R+a_c)] - I_0[q(R+a_c)]K_0(qR)\right] - \kappa q\left[I_1(qR)K_0[q(R+a_c)] + I_0(q[R+a_c])K_1(qR)\right]}\right\} \tag{92}$$

where the variable $\kappa=T_c/M$ is introduced. In the complex p-plane, the function $\eta(r,p)$ is regular at p=0, as can be shown by an expansion of η for small p. This is expected since the limit $p\to 0$ corresponds to the ultimate steady

DOI 10.1007/s10040-015-1252-3

state which is $h(r, +\infty)=0$. $\eta(r,p)$ has a series of single poles on the negative real axis of p which correspond to the p values which nullify the denominator Δ of Eq. (92). The zeros can be expressed as functions of $\beta = \sqrt{-p/D_c}$ using well known relations for Bessel functions of imaginary argument:

$$\Delta(\beta) = \{J_0[\beta R]Y_0[\beta(R+a_c)]-J_0[\beta(R+a_c)]Y_0[\beta R]\}D_c\beta^2 + \{J_0[\beta(R+a_c)]Y_1[\beta R]-J_1[\beta R]Y_0[\beta(R+a_c)]\}\kappa\beta = 0 \quad (93)$$

As previously, the poles p_n corresponding to positive solutions of $\Delta\beta=0$ contribute to the contour integral (as defined in Eq. 69) in order to give a function $k_n(r)\exp(-tD_c/\beta_n^2)$. Here, $k_n(r)$ denotes the residual, i.e. the linear trend of the function $\eta(r,p)$ in the vicinity of the pole $p_n = -\beta_n^2/D_c$. When taking into account the fact that $\Delta\beta_n$=as well as classical relations for Bessel functions (see Carslaw and Jaeger 1959, p. 333), the expression for the residual can be written after some algebra as:

$$k_n(r) = \frac{h_1\kappa\pi}{2R\ln\left(\frac{R+a_c}{R}\right)} \frac{J_0[\beta_n(R+a_c)]Y_0[\beta_n r]-Y_0[\beta_n(R+a_c)]J_0[\beta_n r]}{\frac{\rho_n}{2}-\frac{\beta_n^2}{2\rho_n}\left(\kappa^2+\beta_n{}^2D_c^2-\frac{2\kappa D_c}{R}\right)} \quad (94)$$

where the coefficients ρ_n are defined by:

$$\rho_n = \frac{-\beta_n^2 D_c J_0(\beta_n R)+\kappa\beta_n J_1(\beta_n R)}{J_0[\beta_n(R+a_c)]} \quad (95)$$

The required solution is an infinite series $h(x,t)=\sum_{n=1}^{\infty}k_n(r)\exp(-tD_c/\beta_n^2)$. Only the first major term is retained so that the approximate solution is:

$$h(r,t)\cong k_1(r)\exp\left(-tD_c/\beta_1^2\right) \text{ or } h(r,t)\cong k_1(r)\exp(-t/\tau) \quad (96)$$

β_1 is obtained through an expansion of $\Delta\beta$ in the vicinity of β=0. This requires the expansion of Bessel functions for small values of their argument u which are (here γ is Euler's constant, 0.5772…):

$$J_0(u)\approx 1-(u/2)^2 \quad (97)$$

$$J_1(u)\approx u/2-(u/2)^3/3 \quad (98)$$

$$Y_0(u)\approx 2/\pi\left[\ln(u/2)+\gamma-(u/2)^2\ln(u/2)\right] \quad (99)$$

$$Y_1(u)\approx 2/\pi[-1/u+(u/2)\ln(u/2)+(u/2)(\gamma-1/2)] \quad (100)$$

Using this development for Δ, the evaluation of the smallest solution of $\Delta\beta$=0 is then obtained as:

$$\beta_1\cong\frac{1}{\sqrt{R^2\left[\left(\frac{M}{S_cR}-\frac{1}{2}\right)\ln\left(\frac{R+a_c}{R}\right)+\frac{(R+a_c)^2-R^2}{4R^2}\right]}} \quad (101)$$

For the case of *converging flow*, the aquifer domain is $R - a_c<r<R$. A boundary condition is prescribed at the outlet $r=R - a_c$ as $h(R - a_c)=0$. As previously, the other condition at $r=R$ is a connection to a reservoir with integrated storage $M=a_uS_u$. The function $h(r,t)$ satisfies the same Eq. (86) but, since the flow is now convergent, the mixed boundary condition at $r=R$ is:

$$M\frac{\partial h(R,t)}{\partial t} = -T_c\frac{\partial h(r,t)}{\partial r}\bigg|\, r=R \quad (102)$$

The general solution of the steady-state equation which satisfies $h(R+a_c)=0$ is:

$$h(r) = h_1\frac{\ln[r/(R-a_c)]}{\ln[R/(R-a_c)]} \quad (103)$$

where h_1 is expressed as a function of the initial recharge rate B:

$$h_1 = B\frac{a_uR}{T_c}\ln\left(\frac{R}{R-a_c}\right) \quad (104)$$

 DOI 10.1007/s10040-015-1252-3

The Laplace transform $\eta(r,p)$ of the function $h(r,t)$ yields the associated equation:

$$S_c\left[p\eta - h_1\frac{\ln[r/(R-a_c)]}{\ln[R/(R-a_c)]}\right] = \frac{T_c}{r}\frac{\partial}{\partial r}\left(r\frac{\partial \eta}{\partial r}\right) \quad \text{for } R-a_c < r < R \tag{105}$$

The general solution of Eq. (105) is expressed in terms of modified Bessel functions I_0 and K_0:

$$\eta(x,p) = \frac{h_1}{p}\frac{\ln[r/(R-a_c)]}{\ln[R/(R-a_c)]} + \alpha I_0(qr) + \delta K_0(qr) \tag{106}$$

where α and δ are defined to satisfy the boundary conditions:

$$\eta(x,p) = \frac{h_1}{pR\ln[R/(R-a_c)]}\left\{R\ln\left[\frac{r}{R-a_c}\right] + \frac{\kappa\left[I_0(qr)K_0[q(R-a_c)] - I_0[q(R-a_c)]K_0(qr)\right]}{p\left[-I_0(qR)K_0[q(R-a_c)] + I_0[q(R-a_c)]K_0(qR)\right] - \kappa q\left[I_1(qR)K_0[q(R-a_c)] + I_0[q(R-a_c)]K_1(qR)\right]}\right\} \tag{107}$$

As in the diverging case, the function $\eta(r,p)$ is regular at p=0 and has a series of single poles on the negative real axis of p . These poles are the zeros of the denominator of the last member of Eq. (107). Using standard relations for Bessel functions with an imaginary argument, these zeros are obtained for the values of $\beta = \sqrt{-p/D_c}$ satisfying:

$$\Delta(\beta) = \{-J_0[\beta R]Y_0[\beta(R-a_c)] + J_0[\beta(R-a_c)]Y_0[\beta R]\}D_c\beta^2 + \{J_0[\beta(R-a_c)]Y_1[\beta R] - J_1[\beta R]Y_0[\beta(R-a_c)]\}\kappa\beta = 0 \tag{108}$$

As previously, the poles p_n corresponding to the positive solutions β_n (n=1,2…) of $\Delta(\beta)$=0 contribute to the contour integral (as defined in Eq. 69) via a function $kk_n(r)\exp(-tD_c/\beta_n^2)$. Here $kk_n(r)$ denotes the residual i.e. the linear trend of the function $\eta(r,p)$ in the vicinity of the pole $p_n = -\beta_n^2/D_c$. After some algebra its expression is obtained:

$$kk_n(r) = \frac{h_1\kappa\pi}{2R\ln\left(\frac{R}{R-a_c}\right)} \frac{J_0[\beta_n(R-a_c)]Y_0[\beta_n r] - Y_0[\beta_n(R-a_c)]J_0[\beta_n r]}{\frac{\rho_n}{2} - \frac{\beta_n^2}{2\rho_n}\left(\kappa^2 + \beta_n^2 D_c^2 + \frac{2\kappa D_c}{R}\right)} \tag{109}$$

where the ρ_n are defined by:

$$\rho_n = \frac{-\beta_n^2 D_c J_0(\beta_n R) - \kappa\beta_n J_1(\beta_n R)}{J_0[\beta_n(R-a_c)]} \tag{110}$$

and the required solution is an infinite series $h(r,t) = \sum_{n=1}^{\infty} kk_n(r)\exp(-tD_c/\beta_n^2)$. Only the first major term is retained so that the approximate solution is: $h(r,t) = kk_1(r)\exp(-tD_c/\beta_1^2)$ or $h(r,t) = kk_1(r)\exp(-t/\tau)$.

β_1 is obtained through an expansion of $\Delta\beta$ in the vicinity of β=0 making use of the previous expansion (Eqs. 97–100) of Bessel functions. One obtains the first positive solution of $\Delta\beta$=0 as:

$$\beta_1 \cong \frac{1}{\sqrt{R^2\left[\left(\frac{M}{S_c R} + \frac{1}{2}\right)\ln\left(\frac{R}{R-a_c}\right) - \frac{R^2 - (R-a_c)^2}{4R^2}\right]}} \tag{111}$$

References

Besbes M, Horriche FJ (2007) Définition d'un réseau de surveillance piézométrique du système aquifère du Sahara septentrional [Design of a piezometric monitoring network of the northwestern Sahara aquifer system]. Sécheresse 18(1):13–22

Bredehoeft JD, Neuzil CE, Milly PCD (1983) Regional flow in the Dakota aquifer: a study of the role of confining layers. US Geol Surv Water Suppl Pap 2237-45

Carslaw HS, Jaeger JC (1959) Conduction of heat in solids, 2nd edn. Oxford Univ. Press, Oxford

Chavez A, Davis SN, Sorooshian S (1994) Estimation of mountain front recharge to regional aquifers: 1. development of an analytical hydroclimatic model. Water Res Res 30(7):2157–2167

Custodio E (2002) Aquifer overexploitation: what does it mean? Hydrogeol J 10:254–277. doi:10.1007/s10040-002-0188-6

de Marsily G (1986) Quantitative hydrogeology. Academic, New York

Domenico PA, Schwartz FW (1998) Physical and chemical hydrogeology, 2nd edn. Wiley, New York, 506 pp

Edmunds WM (1999) Integrated geochemical and isotopic evaluation of regional aquifer systems in arid regions. Proc. Int. Conf., Tripoli, Lybia, Regional aquifer systems in arid zones: managing non-renewable resources. IHP-V; Technical Document in Hydrology, UNESCO, Paris

Edmunds WM (2009) Paleoclimate and groundwater evolution in Africa: implications for adaptation and management. Hydrol Sci J 64(4):781–792

Gasse F (2000) Hydrological changes in the African tropics since the last glacial maximum. Quat Sci Rev 19:189–211

Gonçalvez J, Petersen J, Deschamps P, Hamelin B, Baba-Sy O (2013) Quantifying the modern recharge of the "fossil" Sahara aquifers. Geophys Res Lett 40:1–6. doi:10.1002/grl.50478, 2013

Grenier C, Paillou P, Maugis P (2009) Assessment of Holocene surface hydrological corrections for the Ounianga Lake catchment zone (Chad). C R Geosci 341:770–782. doi:10.1016/J.crte.2009.03.004

Habermehl MA (1980) The Great Artesian Basin, Australia. BMR J Aust Geol Geophys 5(1):9–38

Heinl M, Brinkmann PJ (1989) A groundwater model of the Nubian aquifer system. Hydrol Sci J Sci Hydrol 34(4):425–447. doi:10.1080/02626668909491350

Hesse KH, Hissene A, Kheir O, Schnaecker E, Schneider M (1987) Hydrogeological investigations of the Nubian aquifer system, eastern Sahara. Berl Geowiss Abh, Reihe A: Geol Palaeontol 75(2):397–464

Krinner G, Lézine AM, Braconnot P, Sepulchre P, Ramstein G, Grenier C, Gouttevin I (2012) A reassessment of lake and wetland feedbacks on the North African Holocene climate. Geophys Res Lett 39, L07701. doi:10.1029/2012GL050992

Kröpelin S, Verschuren D, Lézine AM, Eggermont H, Cocquyt C, Francus P, Cazet JP, Fagot M, Rumes B, Russell JM, Darius F, Conley DJ, Schuster M, von Suchodoletz H, Engstrom DR (2008) Climate-driven ecosystem succession in the Sahara: the past 6000 years. Science 320(9):765–768. doi:10.1126/science.1154913

Lézine AM, Hély C, Grenier C, Braconnot P, Krinner G (2011) Sahara and Sahel vulnerability to climate changes: lessons from Holocene hydrological data. Quat Sci Rev. doi:10.1016/j.quascirev.2011.07.006

Love AJ, Herczeg AL, Leaney FW, Stadter MF, Dighton JC, Armstrong D (1994) Groundwater residence time and palaeohydrology in the Otway Basin, South Australia: 2H, 18O and 14C data. J Hydrol 153(1):157–187. doi:10.1016/0022-1694(94)90190-2

OSS (2003) Système aquifère du Sahara Septentrional, une conscience de bassin, Observatoire du Sahara et du Sahel [North-western Sahara Aquifer System: a basin awareness—Sahara and Sahel Observatory]. Observatoire du Sahara et du Sahel Boulevard de l'Environnement, Tunis, Tunisia

OSS-UNESCO, ISARM-Africa (2005) Ressources en eau et gestion des aquifères transfontaliers de l'Afrique du Nord et du Sahel [Water resources and management of transborder aquifers in North Africa and the Sahel]. IHP-IV Series on Groundwater no. 11. UNESCO, Paris

Ould Baba Sy M (2005) Recharge et paléorecharge du système aquifère du Sahara septentrional [Recharge and paleorecharge in the north-western Sahara Aquifer System]. PhD Thesis, University of Tunis, Tunisia

Rousseau-Gueutin P, Love AJ, Vasseur G, Robinson HI, Simmons CT, de Marsily G (2013) Time to reach near-steady state in large aquifers. Water Res Res 49:6893–6908. doi:10.1002/wrcr.20534

Scanlon BR, Keese KE, Flint AL, Flint LE, Gaye CB, Edmunds WM, Simmers I (2006) Global synthesis of groundwater recharge in semiarid and arid regions. Hydrol Process 20:3336–3370

Sonntag C (1986) A time-dependent groundwater model for the eastern Sahara. Berl Geowiss Abh, Reihe A 72:124–134

Sonntag C (1999) Assessment methodologies: isotopes and noble gases in Saharan paleowaters and change of groundwater flow pattern in the past. Proc. Int. Conf., Tripoli, Lybia, Regional aquifer systems in arid zones-Managing non-renewable resources, IHP-V Technical Document in Hydrology, UNESCO, Paris

Sonntag C, Thorweihe U, Rudolf J, Loehnert EP, Junghans C, Munnich KO, Klitzsch E, Shazly E, Swailen FM (1980) Paleoclimatic evidence in apparent ^{14}C ages of Saharian ground waters. Radiocarbon 22(3):871–878

Sun AY, Green R, Rodell M, Swenson S (2010) Inferring aquifer storage parameters using satellite and in situ measurements: estimation under uncertainty. Geophys Res Lett 37, L10401. doi:10.1029/2010GL043231

Taylor RG, Koussis AD, Tindimugaya C (2009) Groundwater and climate in Africa: a review. Hydrol Sci J Sci Hydrol 54(4):655–664

Thorweilhe U, Heinl M (2002) Groundwater resources of the Nubian aquifer system NE-Africa. Aquifers of major basins: non renewable water resource. Modified synthesis, Observatoire du Saha et du Sahel, Tunis, 24 pp

Viviroli D, Weingartner R, Messerli B (2003) Assessing the hydrological significance of the world's mountains. Mt Res Dev 23(1):32–40. doi:10.1659/02764741(2003)023[0032:ATHSOT]2.0.CO;2

Viviroli D, Dürr H, Meybeck M, Messerli B (2007) Mountains of the world: water towers for humanity—typology, mapping and global significance. Water Res Res 43:W07447. doi:10.1029/2006WR005653

Wilson J, Guam H (2000) Mountain-block hydrology and mountain-front recharge. In: Phillips FM, Hogan J, Scanlon B (eds) Groundwater recharge in a desert environment: the Southwestern United States. AGU, Washington, DC